RACE for 2030

RELIABLE
AFFORDABLE
CLEAN
ENERGY

FINAL REPORT

Understanding power system dynamics with high levels of grid-forming inverters



Final report

RACE for Network Program

Understanding power system dynamics with high levels of grid-forming inverters

Project Code: 22.N2.S.0481

Citations

Abbasi, M., Dargahi, M., Ghosh, A., Harjula, A., Mishra, Y., Paice, K., Zhang, Y. (2026). 22.N2.S.0481: Understanding power system dynamics with high levels of grid-forming inverters. Prepared for RACE for 2030.

Project team

Queensland University of Technology

- Maysam Abbasi
- Yuchen Zhang
- Yateendra Mishra

Curtin University

- Arindam Ghosh

Powerlink

- Kevin Paice
- Mahdi Dargahi
- Antti Harjula

Project partners

Acknowledgement of Country

The authors of this report would like to respectfully acknowledge the Traditional Owners of the ancestral lands throughout Australia and their connection to land, sea and community. We recognise their continuing connection to the land, waters, and culture and pay our respects to them, their cultures and to their Elders past, present, and emerging.

What is RACE for 2030?

RACE for 2030 is a 10-year cooperative research centre (CRC) with $350 million of resources to fund and support research towards a reliable, affordable, and clean energy future.

Disclaimer

The authors have used all due care and skill to ensure the material is accurate as at the date of this report. The authors do not accept any responsibility for any loss that may arise by anyone relying upon its contents.

Executive summary

The increasing penetration of inverter-based renewable generation is changing the dynamic behaviour of modern power systems and reducing the support traditionally provided by synchronous machines for frequency and oscillation control. Grid-following renewable interfaces may satisfy steady-state operating requirements. However, under severe disturbances, they can provide only limited dynamic support. In some cases, they may introduce stability challenges, especially in low-inertia networks. In contrast, grid-forming inverters (GFMs) can establish voltage and frequency while also emulating aspects of synchronous-machine behaviour. This feature enables them to contribute to damping during disturbances. This project addresses the need for improved modelling and evaluation of GFMs in Australian networks.

This project was motivated by the need to improve understanding of how GFMs should be modelled, analysed, and deployed in Australian power systems. Specifically, the project addressed three linked practical questions. First, how does the increasing penetration of inverter-based resources affect oscillatory behaviour when synchronous support is displaced? Second, how can GFM models be represented, validated, and tuned so that their dynamic behaviour can be evaluated with confidence? Third, in larger interconnected systems, do the benefits of GFMs depend only on the number of devices employed, or must other factors, such as parameter tuning, electrical location, and modal participation, also be considered?

To address these questions, the project progressed through several modelling and analysis stages. The work began with baseline renewable-integration studies in a simplified 14-generator Australian/NEM model. It then proceeded to the use, assessment, and validation of the REGFM_B1 grid-forming inverter model. This was followed by benchmark studies using SMIB and Kundur systems, before the analysis was extended to multiple-GFM placement studies in the simplified 14-generator NEM model. Across these stages, PSSE, DSATools, and PowerWorld Simulator were used together with Python, MATLAB, and automation workflows to support steady-state, transient, eigenvalue, and modal analyses.

The results show that increasing renewable penetration without equivalent dynamic support can worsen post-disturbance oscillatory behaviour. In contrast, appropriately tuned GFMs can improve damping and dynamic performance. In addition, the studies show that these benefits do not depend on device count alone. They also depend on network strength, controller settings, and GFM placement relative to dominant inter-area oscillation patterns. In the simplified 14-generator NEM system, representative placement studies indicated that GFMs can provide stronger damping improvement when located at electrically influential locations associated with the selected inter-area mode examined through GFM placements in NSW and QLD. Damping improvement was weaker when these devices were concentrated at weakly participating locations. The multiple-GFM studies further showed that, for the selected inter-area mode, damping improvement was clearer when GFMs were placed to influence the dominant modal structure, rather than being concentrated within one area or selected

only by device count. Overall, these results show that successful GFM deployment depends not simply on device count, but on whether the devices reshape the dominant modal structure of the system.

Overall, this project has established a strong technical basis for evaluating GFMs in modern and low-inertia power systems. It has developed a modelling and analysis workflow and generated validated insights into GFM parameter tuning and system-strength dependence. These findings are relevant to Australia's energy transition and to the secure integration of inverter-based renewable generation.

Contents

EXECUTIVE SUMMARY 3

1. PROJECT PROGRESS 6

1.1 Research activities and technical progress 6

1.2 Data and sources used in the project 7

1.3 Key findings 8

1.4 Research gaps and limitations 9

1.5 Issues and difficulties encountered, if any, during the course of the research activities 10

1.6 Actions proposed or undertaken to overcome the issues and difficulties 10

2. IRG AND STAKEHOLDER WORKSHOPS 11

3. CONCLUSIONS AND NEXT STEPS 12

3.1 Conclusions 12

3.2 Response to project objectives 13

3.3 Value of findings 13

3.4 Next steps 13

4. REFERENCES 15

5. GLOSSARY 16

6. APPENDIX 18

6.1 Supplementary Technical Figures and Tables by Project Stage 18

1. Project Progress

1.1 Research activities and technical progress

The project began with the development and refinement of a simplified 14-generator Australian/NEM model in PSSE. In this stage, selected synchronous generators were replaced by available generic converter-interfaced wind and photovoltaic renewable models. This established a baseline understanding of how increasing inverter-based renewable penetration affects steady-state and post-disturbance behaviour. The steady-state responses remained broadly acceptable. However, as shown in Figures A1.2–A1.4 and Table A1.1, post-fault oscillatory behaviour worsened as more synchronous generators were replaced by converter-interfaced wind and PV generation. It should be noted that Python automation was developed to support scenario generation and simulation analysis. This phase established the initial PSSE-based Australian/NEM study platform and the dynamic problem context for the later GFM studies.

The research then moved toward explicit modelling of grid-forming inverter behaviour using a SMIB benchmark in DSATools, in consultation with the IRG. This stage focused on steady-state verification, transient studies, and iterative refinement of inverter control structures. It also included work on low-voltage and fault-related behaviour. Practical issues were identified in transient simulation and controller implementation. These issues led to repeated model refinement. This step was important because it provided a controlled benchmark environment. In this environment, inverter behaviour could be isolated, tested, and improved before moving to broader benchmark and system-level studies. The supporting results for this transition and early GFM modelling stage are provided in Appendix A.2 and Appendix A.3, including Figures A2.1–A2.2, Table A2.1, Figures A3.1–A3.2, and Table A3.1.

The next major stage centred on the use, assessment, and validation of the REGFM_B1 grid-forming inverter model. SMIB studies in PowerWorld Simulator and DSATools were used to examine the effects of short-circuit ratio, line impedance, and virtual inertia on oscillation frequency and damping. These results are illustrated in Figures A4.2–A4.4 and summarised in Table A4.1. Grid-strength cases ranged from SCR 6.25 down to 1.0. Both small disturbances and three-phase bus faults were considered. This stage supported systematic small-signal and time-domain studies using a validated REGFM_B1 modelling workflow. Further supporting results for the REGFM_B1 validation studies are provided in Appendix A.5, including Figures A5.1–A5.6 and Table A5.1.

The work then expanded to the Kundur two-area benchmark system. This stage combined time-domain simulation, eigenvalue analysis, and matrix-pencil-based mode extraction. These methods were used to compare GFM and synchronous-generator behaviour. They were also used to derive a tuning approach for approximate equivalence between REGFM_B1 and GENROU under selected conditions, as shown in Figure A6.2. The same stage examined the effects of inertia and damping parameters. Multi-GFM interaction studies were then performed in Kundur using several parameter sets and placement combinations. The main parameter-sensitivity and placement outcomes are summarised in Table A6.1. This analysis moved the project from SMIB-based and single-device benchmarking to a standard multi-machine oscillation problem. It allowed the project team to study inter-area effects and placement

interactions more meaningfully. The detailed tuning, equivalence, parameter-sensitivity, and Kundur placement results are presented in Appendix A.6, including Figures A6.1–A6.9 and Table A6.1.

The project then investigated the simplified 14-generator NEM model. This stage focused on multiple-GFM placement across Area 2 (NSW) and Area 4 (QLD) buses. Using PowerWorld Simulator, SimAuto, MATLAB, and automation workflows, the project evaluated a range of placement patterns. It also analysed the dominant inter-area modes using participation, phase-angle clustering, and generator opposition measures. Representative best-versus-worst placement outcomes are shown in Figures A7.4–A7.5 and summarised in Table A7.2. This was the most deployment-oriented stage of the work. It translated the earlier benchmark findings into an Australian-relevant power-system setting. The detailed multiple-GFM placement results are provided in Appendix A.7, including Figures A7.3–A7.18 and Tables A7.1–A7.4.

The overall progression of the project activities is summarised in Figure 1.

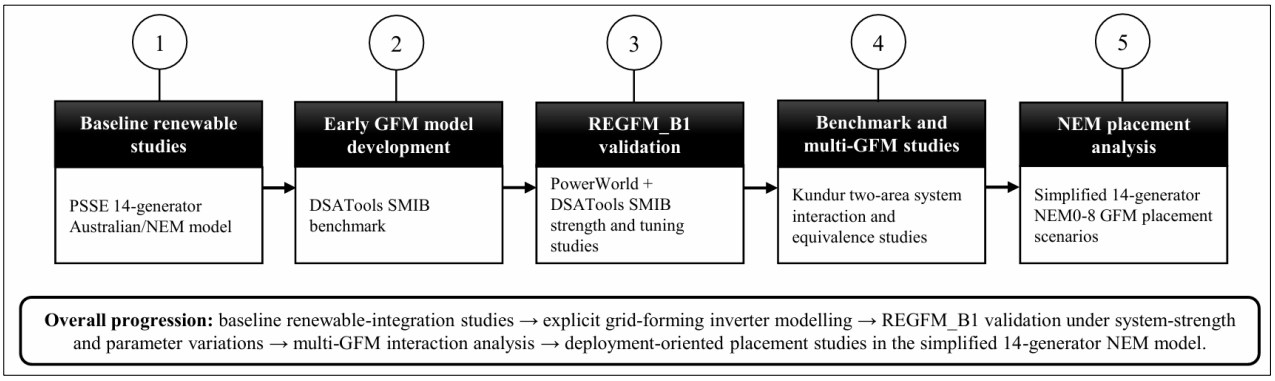


Figure 1. Project workflow, from PSSE-based baseline studies to SMIB, Kundur, and simplified 14-generator NEM multiple-GFM placement studies.

1.2 Data and sources used in the project

The project used benchmark and partner-supported study systems, and the main system-level platform was the simplified 14-generator Australian/NEM model implemented in PSSE and PowerWorld Simulator. For the final-stage multiple-GFM placement studies, the study system was selected from the six available simplified 14-generator system versions reported by Gibbard and Vowles in [1]. A SMIB benchmark model in DSATools was used for early GFM modelling and validation. The Kundur two-area system was used as a standard benchmark for inter-area oscillation studies. Across these systems, the project analysed steady-state results, transient responses, eigenvalues, modal frequencies, damping ratios, participation patterns, and placement comparisons.

The software environments used in the project were PSSE, DSATools, and PowerWorld Simulator, while Python, MATLAB, and SimAuto were used to support scenario generation, result extraction, automation, and comparative analysis. Accordingly, the project data were primarily simulation-based, and the resulting dataset consisted of model outputs under defined operating points, parameter sets, grid-strength conditions, disturbance cases, and GFM placement scenarios.

1.3 Key findings

The first main finding is that increased renewable penetration can worsen disturbance-related oscillatory behaviour when synchronous support is displaced without equivalent dynamic support. This was established in the early 14-generator studies. Based on the results, steady-state performance remained broadly acceptable but post-disturbance oscillatory behaviour became less satisfactory as more synchronous generators were replaced by converter-interfaced wind and PV generation (Figures A1.2–A1.4 and Table A1.1). This deterioration in oscillatory behaviour remains the key motivation for the project.

The second key finding is that GFMs based on REGFM_B1 can provide strong damping support and improve dynamic performance when appropriately tuned and deployed [2, 3]. The benchmark studies report satisfactory transient and small-signal performance of the REGFM_B1 model, and the broader project results show damping improvement across the studied benchmark and system-level cases.

The third finding is that GFM behaviour depends on system strength. In the SMIB studies, changes in line impedance and SCR affected both damping ratio and oscillation frequency. For the mode reported in Figure A4.4, increasing virtual inertia at fixed line reactance reduced both damping ratio and natural frequency. At fixed H, reducing line reactance increased natural frequency but reduced damping ratio. These findings highlight the need to interpret network strength and controller settings together, as summarised in Table A4.1.

The fourth significant finding is that controller-parameter effects are systematic. In SMIB and Kundur studies, increasing virtual inertia (H) generally reduced damping and frequency [2, 3]. Moreover, increasing the main damping term (D_1) generally improved damping while reducing frequency, although the Kundur damping response was not monotonic over the full range shown in Figure A6.4 [2, 3]. However, increasing the secondary damping term (D_2) produced only minor changes [2, 3]. These findings are summarised in Table A6.1 and illustrated in Figure A6.4. These results indicate that GFM performance depends on coordinated tuning rather than on high virtual inertia alone.

Another important outcome concerns the relationship between GFM and synchronous-generator behaviour. REGFM_B1 can be tuned to approximately match selected modal behaviour of a synchronous generator, as shown by the tuning approach in Figure A6.2. However, this equivalence is valid only under selected conditions. If the operating condition changes, the GFM parameters may need to be re-tuned. This means that synchronous-machine behaviour can provide useful guidance, but GFM behaviour should not be treated as universally identical to conventional synchronous-machine dynamics.

The sixth and most practically significant finding is that multiple GFMs can improve damping, but placement matters more than number alone. In the Kundur system, the baseline case had 10.2% damping at 0.671 Hz. One GFM increased damping to about 15.9–18.8%. The best two-GFM symmetric cross-area placement reached 40.9% damping. By contrast, the weakest same-area placement reached

only 18.6% (Table A6.1). The 14-generator NEM results show a similar principle in an Australian-relevant setting. Damping improvement was strongest when GFMs were placed at electrically influential locations that reshaped the dominant inter-area mode. Weakly participating placements left the modal structure close to baseline (Table A7.2). The results also suggest that distributing GFMs across both NSW and QLD can be more effective than concentrating them within one area, provided that the selected buses are electrically influential for the dominant inter-area mode.

Taken together, these findings show that the strongest damping gains occur when GFMs are placed at locations that reshape the dominant inter-area mode, rather than being selected only by device count. More broadly, the dynamic value of GFMs depends on modal participation, electrical location, and controller tuning, not only on the number of devices installed.

1.4 Research gaps and limitations

Although the project has established a strong technical workflow and produced consistent trends across several systems, some important limitations remain. First, the larger-system studies were conducted on a simplified 14-generator Australian/NEM model rather than on the full NEM. This was appropriate for research benchmarking and controlled comparison, but it means the results should be interpreted as planning-oriented and deployment-guiding insights rather than as direct operational prescriptions for the full network. In particular, the simplified model does not capture all network details, operating constraints, protection settings, control interactions, and regional operating conditions that would be present in a full-NEM operational study.

Second, not all inter-area modes, disturbance locations, and parameter combinations could be exhaustively examined within the project scope. The project focused on selected representative modes, disturbance cases, parameter settings, and GFM placement scenarios to identify clear technical trends. The latest workshop outcomes identified the need to extend analysis across additional inter-area modes and examine selected combinations involving synchronous condensers and GFM-BESS arrangements. These extensions would help test whether the observed placement and tuning trends remain consistent across a wider range of system conditions.

Third, the cross-platform studies showed broadly consistent trends across PSSE, DSATools, and PowerWorld, which increased confidence in the main findings. Some discrepancies were observed in detailed GFM-related damping behaviour and higher-frequency control-related modes. These discrepancies are expected in detailed dynamic studies and reinforce the need for careful model validation and controller interpretation in future planning or operational studies.

Fourth, the project has shown that damping ratio alone is not sufficient for interpreting larger-system multi-GFM behaviour. As the work progressed from single-device to multi-placement studies, meaningful interpretation required participation patterns, angle clustering, generator opposition measures, and modal-structure analysis. This means that future GFM placement studies should

consider not only whether damping improves, but also how the dominant mode shape, participating generators, and inter-area relationships are changed by the selected GFM locations.

1.5 Issues and difficulties encountered, if any, during the course of the research activities

The project encountered several technical challenges. In the early 14-generator renewable studies, wind and PV representations produced convergence and dynamic-simulation issues that required refinement before the results could be used confidently.

A second challenge was the configuration and validation of GFM models in DSATools and related environments. Project records identified transient-simulation errors and multiple iterations in establishing a stable and analytically useful GFM representation. This progression is shown through the original and refined fault-capable versions in Figures A3.1–A3.2 and Table A3.1.

A third challenge was the need to reconcile results across PSSE, DSATools, and PowerWorld Simulator. Cross-tool comparisons were broadly consistent, but some discrepancies were observed, especially when interpreting model-dependent damping behaviour.

A final challenge emerged in the larger-system multi-GFM studies. As the project moved from single-device analysis to multiple-placement scenarios, damping ratios alone were insufficient for interpretation. Meaningful assessment required modal participation, angle clustering, and system-structure analysis.

1.6 Actions proposed or undertaken to overcome the issues and difficulties

Several measures were taken to address these issues. Python automation was introduced in the early PSSE studies to improve repeatability, reduce manual setup errors, and support consistent comparison across large numbers of scenarios.

To resolve inverter-model and transient-simulation difficulties, the project progressively improved the modelling workflow and validated the REGFM_B1 model for SSAT and TSAT studies. Earlier project documentation notes that DSATools transient issues were partly resolved by modifying inverter models and simulation parameters, while later project updates report satisfactory transient and small-signal behaviour of the REGFM_B1 model.

To improve confidence in the results, the project used cross-validation across PSSE, DSATools, and PowerWorld Simulator and applied complementary analytical methods, including transient simulation, eigenvalue analysis, and matrix-pencil mode extraction.

To improve practical relevance and scalability, the project deliberately expanded from baseline renewable studies to SMIB and Kundur benchmarks and then to the simplified 14-generator NEM model. Further extensions could examine additional inter-area modes, fault locations, parameter combinations, and selected combinations involving synchronous condensers and GFM-BESS arrangements.

2. IRG and Stakeholder Workshops

IRG and stakeholder participation included representatives from Powerlink, Ausgrid, and RACE for 2030, together with the QUT project team.

The workshops helped guide the project from broad renewable-integration concerns toward a more focused and technically useful investigation of grid-forming inverter dynamics. Early discussions supported the use of a simplified Australian/NEM benchmark and confirmed that dynamic behaviour under faults was a more critical issue than steady-state feasibility alone.

As the work matured, the workshops supported the transition to benchmark-system studies in SMIB and Kundur configurations, the explicit use and validation of REGFM_B1, and deeper analysis of controller tuning, system strength, and modal behaviour. Later project directions, including the extension of the 14-generator NEM analysis across multiple modes and fault locations, were also shaped through these discussions.

The later workshop-informed stages were especially important since they shifted the project from asking whether GFMs improve damping to asking where they should be placed and how they should be tuned to improve inter-area modes in Australian-relevant networks. This represented a move from model validation toward deployment-oriented guidance for planning and operation.

The workshops therefore contributed in three main ways. First, they improved technical relevance by aligning the research questions with practical industry concerns. Second, they improved model-validation quality by testing the evolving results against external feedback. Third, they helped move the project from model validation toward deployment-oriented interpretation that is more useful for planners, operators, and stakeholders interested in future GFM deployment strategies. The overall milestone progression shaped through these activities is summarised in Figure 2.

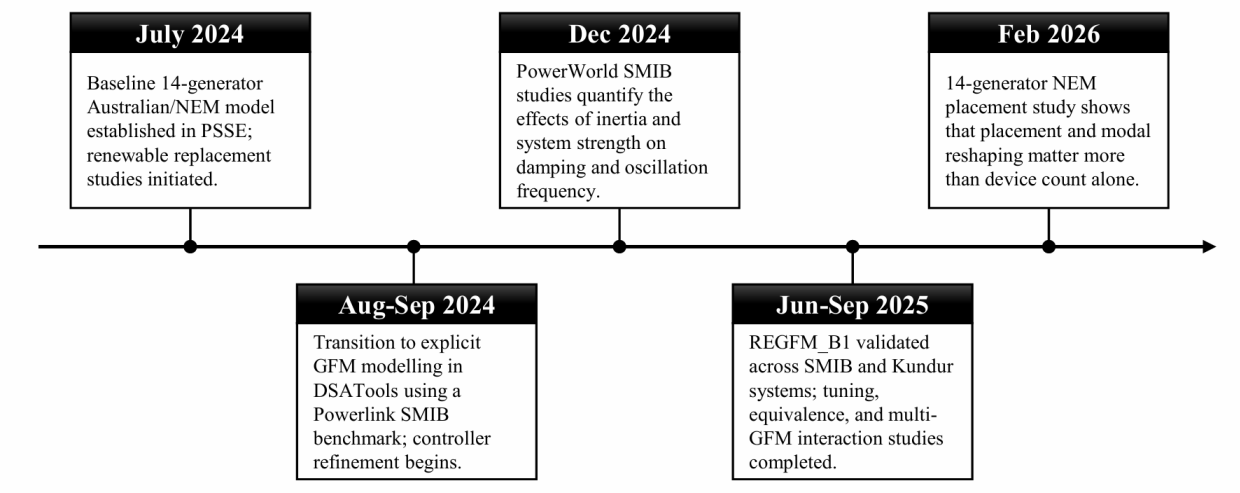


Figure 2. Project milestone progression, from PSSE-based renewable-integration studies to multiple-GFM placement analysis in the simplified 14-generator NEM model.

3. Conclusions and Next Steps

3.1 Conclusions

This project has shown that the displacement of synchronous generation by inverter-based renewable generation can worsen oscillatory behaviour if equivalent dynamic support is not provided. It has also shown that appropriately tuned GFMs can provide meaningful damping support across benchmark and Australian-relevant study systems.

The project developed and validated a practical workflow for GFM analysis using PSSE, DSATools, PowerWorld Simulator, Python, MATLAB, and SimAuto. Through this workflow, the project established that GFM behaviour depends strongly on system strength, controller tuning, and electrical location. The studies further showed that high virtual inertia alone is not a sufficient design principle; tuning must balance damping improvement against slower oscillatory response and other control effects.

Most importantly, the project showed that in larger systems, the benefit of GFMs depends more on placement and modal influence than on the number of units alone. In both Kundur and the simplified 14-generator NEM model, the strongest improvements occurred when GFMs were placed at electrically influential locations that materially changed the dominant inter-area mode. This was the project's main deployment-oriented conclusion.

Detailed discussion of selected results from this project is presented in [2] and [3], where these findings are reported in greater depth.

3.2 Response to project objectives

The first project objective was to develop tools for evaluating the impact of GFMs across electricity networks. This objective was met through the development of a multi-platform modelling and analysis workflow covering baseline renewable studies, benchmark GFM validation, tuning studies, and multi-placement analysis.

The second project objective was to use the developed tools to assist in the operation and control of GFMs for secure power-system operation. This objective was addressed by producing practical findings on system-strength dependence, parameter tuning, approximate equivalence with synchronous generators under selected conditions, and location-dependent damping benefit in larger systems.

The third project objective was to address technical capability needs relevant to industry. This objective was addressed through model validation, cross-platform comparison, benchmark studies, and structured interaction with industry and stakeholder participants throughout the project.

3.3 Value of findings

For network planners and operators, the project provides a clear analytical message: GFM deployment should be evaluated in relation to inter-area mode structure. Electrically influential locations, including interface locations where relevant, can provide materially greater damping benefit than less influential locations.

For investors in GFM-capable BESS, the project indicates that the system-level damping contribution of an installation is location-dependent. A GFM-capable BESS placed where it participates strongly in the dominant oscillation mode is likely to deliver greater system-level damping benefit than one placed at a weakly participating location. This should be interpreted as a technical planning insight rather than as a direct commercial forecast.

For market and system operators, the project provides evidence that GFM placement and tuning can materially influence oscillatory performance in low-inertia settings following disturbances. The findings are therefore relevant to future secure-operation frameworks in systems with increasing inverter-based penetration.

3.4 Next steps

Future work could extend the simplified 14-generator NEM analysis across additional relevant inter-area modes, compare the impact of disturbance location more systematically, investigate additional virtual inertia and damping settings, and examine scenarios involving synchronous condensers and combined GFM-BESS arrangements.

Further work could also improve consistency across simulation tools and refine the interpretation of control-related modes so that future studies can be translated more confidently from benchmark systems to broader Australian network applications.

4. References

[1] Gibbard, Mike, and David Vowles. "Simplified 14-generator model of the South East Australian power system." *The University of Adelaide, South Australia* 18 (2014): 1-38.

[2] M. Abbasi, Y. Zhang, F. Zare, A. Ghosh and Y. Mishra, "Impact of Virtual-Inertia-Based Grid-Forming Inverters on Power System Oscillations," 2025 IEEE International Conference on Energy Technologies for Future Grids (ETFG), Wollongong, Australia, 2025, pp. 1–6, doi: 10.1109/ETFG61999.2025.11402463.

[3] M. Abbasi, Y. Zhang, F. Zare, et al., "Impact of Grid-Forming Inverters equipped with Virtual Inertia on Power System Stability: An Eigenvalue and Dynamic Simulation Study," 2025 IEEE Power & Energy Society General Meeting (PESGM), Austin, TX, USA, 2025, pp. 1-5, doi: 10.1109/PESGM52009.2025.11474681.

5. Glossary

AEMO	Australian Energy Market Operator
AVR	Automatic Voltage Regulator
BESS	Battery Energy Storage System
CER	Customer Energy Resources
DSATools	Dynamic Security Assessment Tools
ETFG	IEEE International Conference on Energy Technologies for Future Grids
GENCLS	Classical synchronous generator model
GENROU	Round-rotor synchronous generator model
GFI	Grid-forming inverter
GFL	Grid-following
GFM	Grid-forming
IBR	Inverter-based resource
IRG	Industry Reference Group
NEM	National Electricity Market
NSW	New South Wales
PoC	Point of Connection
PSS	Power System Stabiliser
PSAT	Powerflow & Short-Circuit Analysis Tool
PSSE	Power System Simulator for Engineering
PWS / PowerWorld	PowerWorld Simulator
QLD	Queensland
REGFM_B1	The grid-forming inverter model used and validated in this project
RES	Renewable Energy Sources
SCR	Short-Circuit Ratio
SG	Synchronous generator
SimAuto	PowerWorld automation interface
SMIB	Single-Machine Infinite-Bus
SSAT	Small-signal stability analysis tool/module in DSATools

Syn Con / SynCons	Synchronous condenser(s)
TSAT	Transient stability analysis tool/module in DSATools
UDM	User-defined model
VSM	Virtual synchronous machine

6. APPENDIX

6.1 Supplementary Technical Figures and Tables by Project Stage

This appendix presents selected supporting figures and tables by project stage so that the technical progression of the research can be followed clearly, from baseline renewable-integration studies in the simplified Australian/NEM model to benchmark-system validation and finally to deployment-oriented multiple-GFM placement analysis. The appendix is intended not only to document results, but also to explain at the start of each subsection how that stage contributed to the project's final conclusions.

A.1 Baseline Renewable-Integration Studies in the Simplified Australian/NEM Model

This stage established the initial simulation platform for the project. The work focused on the simplified 14-generator Australian/NEM model in PSSE and examined the impact of replacing selected synchronous generation with available generic converter-interfaced wind- and PV-based renewable resources, treated here as grid-following rather than grid-forming. The main result was that steady-state operation remained broadly acceptable, but post-disturbance oscillatory behaviour became less satisfactory as renewable penetration increased. This stage is important because it provides the baseline motivation for the later grid-forming inverter studies: the key issue was not power-flow feasibility alone, but the deterioration of dynamic performance as synchronous support was displaced.

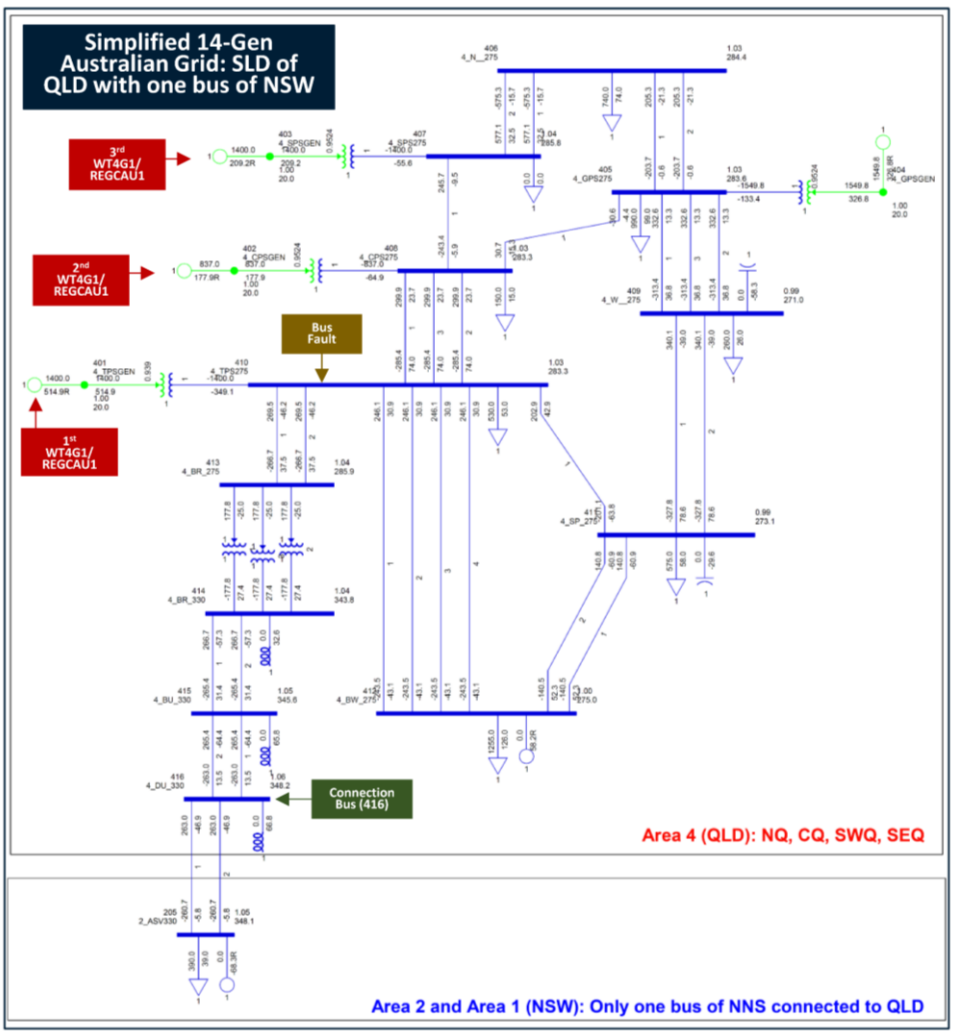


Figure A1.1. PSSE-based simulation model of the simplified 14-generator Australian/NEM system for cases with zero to three renewable units.

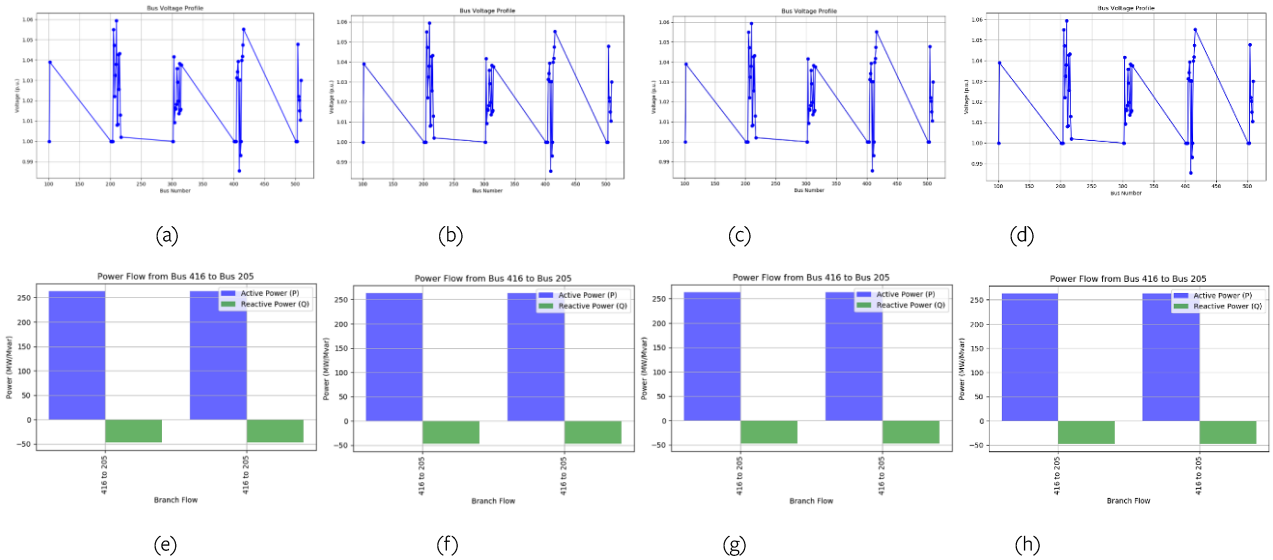


Figure A1.2. Comparison of steady-state responses in the simplified 14-generator NEM model for cases with different numbers of synchronous generators replaced by converter-interfaced wind generation: (a) baseline case without generator replacement, bus-voltage profile; (b) one WT4G1 unit at Bus 402, bus-voltage profile; (c) two WT4G1 units at Buses 401 and 402, bus-voltage profile; (d) three WT4G1 units at Buses 401-403, bus-voltage profile; (e) baseline case without generator replacement, power flow (MW and MVar); (f) one WT4G1 unit at Bus 402, power flow (MW and MVar); (g) two WT4G1 units at Buses 401 and 402, power flow (MW and MVar); and (h) three WT4G1 units at Buses 401-403, power flow (MW and MVar).

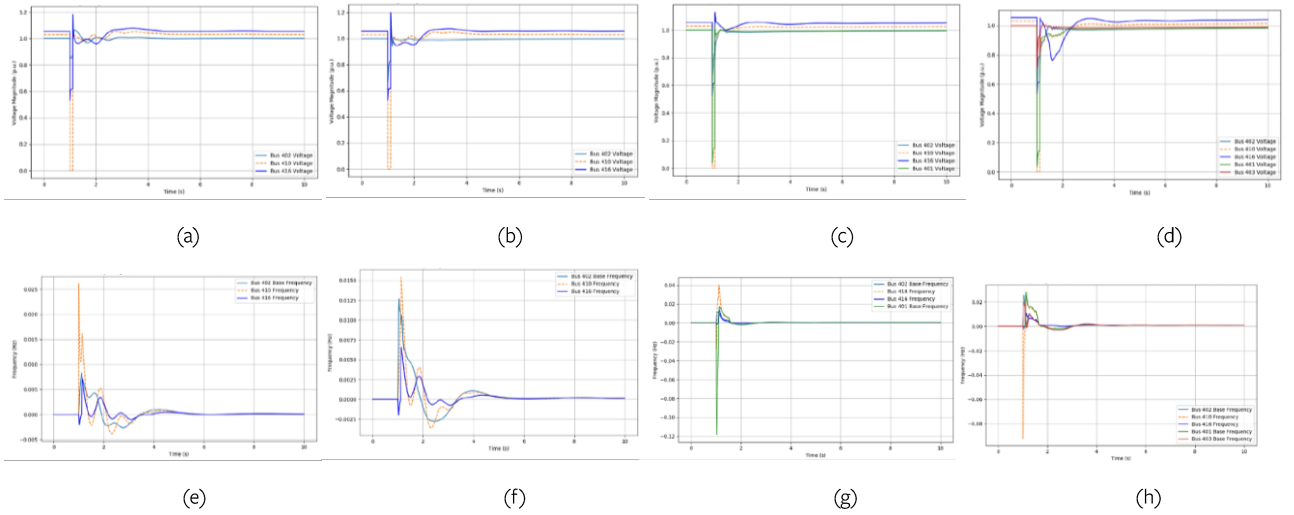


Figure A1.3. Comparison of dynamic responses in the simplified 14-generator NEM model for cases with different numbers of synchronous generators replaced by converter-interfaced wind generation: (a) baseline case without generator replacement, voltage magnitude (p.u.); (b) one WT4G1 unit at Bus 402, voltage magnitude (p.u.); (c) two WT4G1 units at Buses 401 and 402, voltage magnitude (p.u.); (d) three WT4G1 units at Buses 401-403, voltage magnitude (p.u.); (e) baseline case without generator replacement, system frequency (Hz); (f) one WT4G1 unit at Bus 402, system frequency (Hz); (g) two WT4G1 units at Buses 401 and 402, system frequency (Hz); and (h) three WT4G1 units at Buses 401-403, system frequency (Hz).

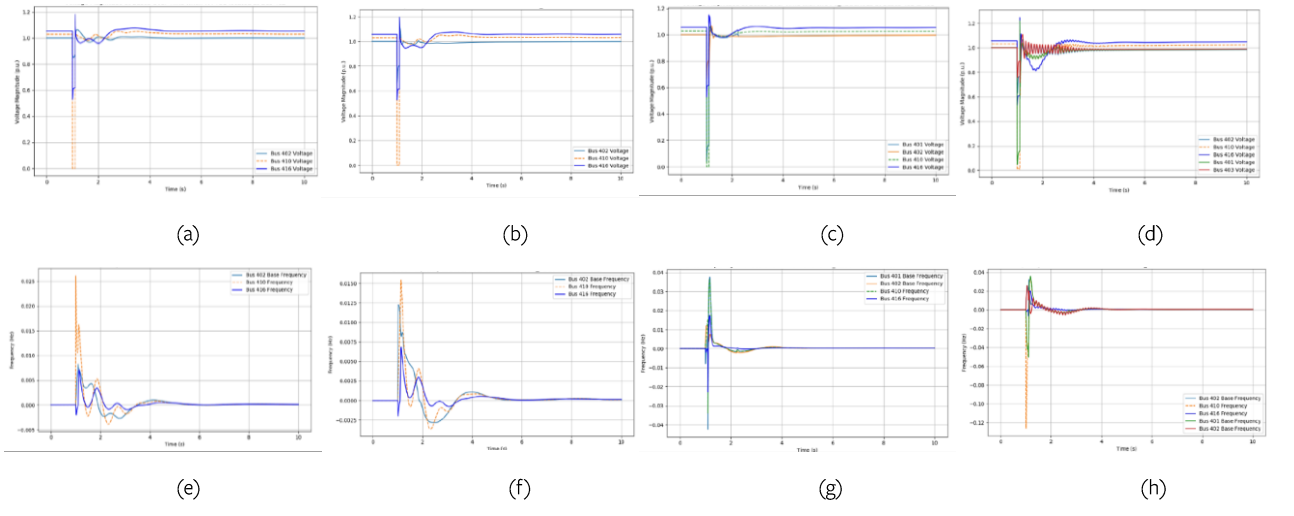


Figure A1.4. Comparison of dynamic responses in the simplified 14-generator Australian/NEM model for cases with different numbers of synchronous generators replaced by converter-interfaced PV generation: (a) baseline case without generator replacement, voltage magnitude (p.u.); (b) one REGCAU1 unit at Bus 402, voltage magnitude (p.u.); (c) two REGCAU1 with REECAU1 units at Buses 401 and 402, voltage magnitude (p.u.); (d) three REGCAU1 with REECAU1 units at Buses 401-403, voltage magnitude (p.u.); (e) baseline case without generator replacement, system frequency (Hz); (f) one REGCAU1 with REECAU1 unit at Bus 402, system frequency (Hz); (g) two REGCAU1 with REECAU1 units at Buses 401 and 402, system frequency (Hz); and (h) three REGCAU1 with REECAU1 units at Buses 401-403, system frequency (Hz).

Table A1.1. Scenarios involving the replacement of synchronous generators with converter-interfaced wind and PV generation considered in the initial PSSE-based study.

Scenario	Replacement model	Bus locations / configuration	Study type	Main observation
Base case	No replacement	Original 14-generator system	Steady-state and dynamic	Reference case used for comparison
Case 1	One WT4G1/ REGCAU1 with REECAU1	One selected replacement location in the study system	Steady-state and dynamic	Steady-state performance remained acceptable; post-fault oscillations increased relative to the base case
Case 2	Two WT4G1/ REGCAU1 with REECAU1 units	Two selected replacement locations in the study system	Steady-state and dynamic	Oscillatory deviation increased further after the disturbance
Case 3	Three WT4G1/ REGCAU1 with REECAU1 units	Three selected replacement locations in the study system	Steady-state and dynamic	Largest post-fault oscillatory deviation among the tested cases involving the replacement of synchronous generators with wind or PV generation.

A.2 Transition from Baseline Renewable Studies to Early GFM Modelling

This stage is important because it bridges the initial PSSE renewable studies and the later, more explicit GFM work. It includes both continued PSSE-based studies with wind and PV models and the first DSATools-based SMIB benchmark studies involving a grid-forming inverter representation. The main outcome of this stage was that the project moved from identifying the dynamic problem caused by the increasing replacement of synchronous generation with converter-interfaced wind and PV generation to beginning a controlled analytical investigation of GFM-based dynamic support.

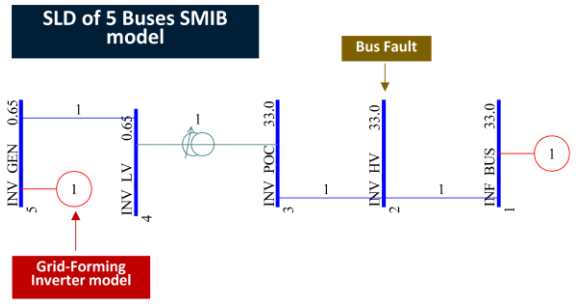
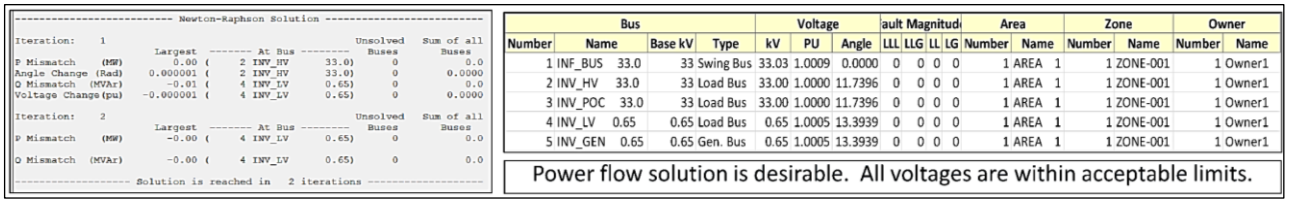
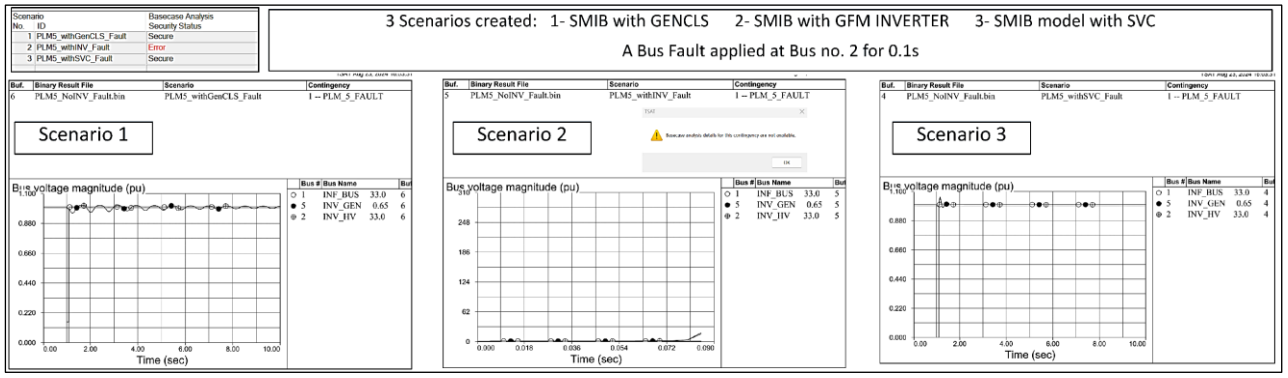


Figure A2.1. DSATools-based SMIB benchmark used for early grid-forming inverter analysis.



(a)



(b)

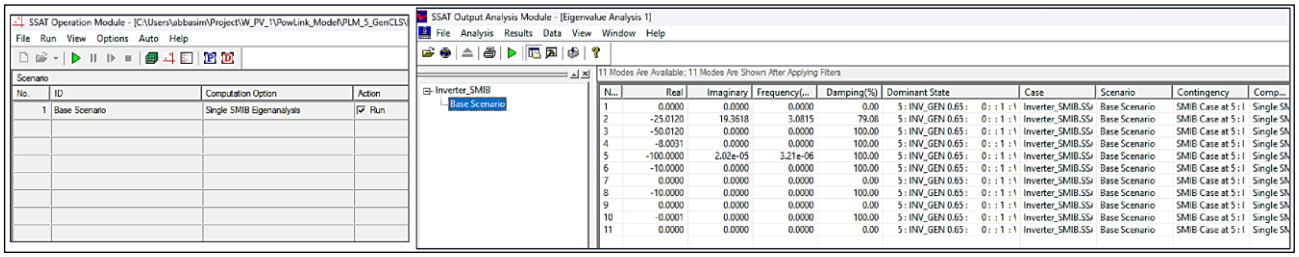
Figure A2.2. Early DSATools results for the SMIB benchmark: (a) PSAT steady-state analysis; and (b) TSAT transient-stability analysis for three scenarios (SMIB with GENCLS, GFM, and SVC).

Table A2.1. Summary of the August 2024 study streams and key outcomes.

Study stream	System / model	Software	Cases considered	Main outcome
Wind integration study	Simplified 14-generator Australian/NEM model	PSSE	Base case and cases replacing synchronous generators with WT4G1 wind models	Steady-state operation remained acceptable, but dynamic oscillations increased as more synchronous generators were replaced by converter-interfaced wind generation.
PV integration study	Simplified 14-generator Australian/NEM model	PSSE	Base case and cases replacing synchronous generators with REGCAU1-based PV models	Renewable integration scenarios were successfully established for further comparison of steady-state and post-disturbance behaviour.
Early GFM benchmark study	5-bus / SMIB benchmark system	DSATools	GENCLS, GFM inverter, and SVC cases	Power-flow solution was acceptable and transient benchmarking of the GFM representation was initiated
Project transition outcome	Australian/NEM model + SMIB benchmark	PSSE + DSATools	Renewable studies and early inverter studies	The project moved from analysing the replacement of synchronous generation with converter-interfaced renewable generation toward explicit investigation of grid-forming inverter dynamics.

A.3 Refinement of the GFM Model in DSATools

This stage documents the first substantial refinement of the GFM representation. The presentation shows both the original and modified versions of the SMIB model provided by Powerlink, including PSAT, TSAT, and SSAT results, and introduces low-voltage- and fault-related improvements. The main result of this stage was that the GFM representation progressed from an initial workable benchmark model to a more robust model with improved transient and fault-related behaviour, making it more suitable for later systematic analysis.

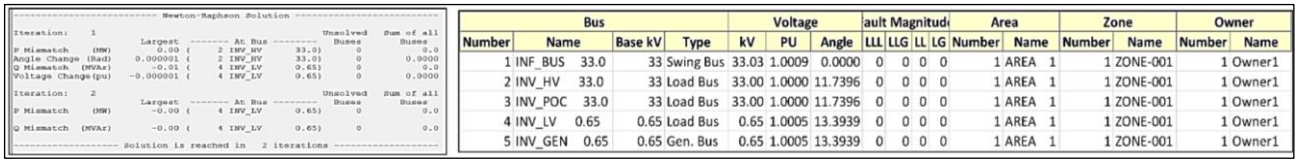


(a)



(b)

Figure A3.1. Results of the original GFM model in (a) PSAT and (b) SSAT.



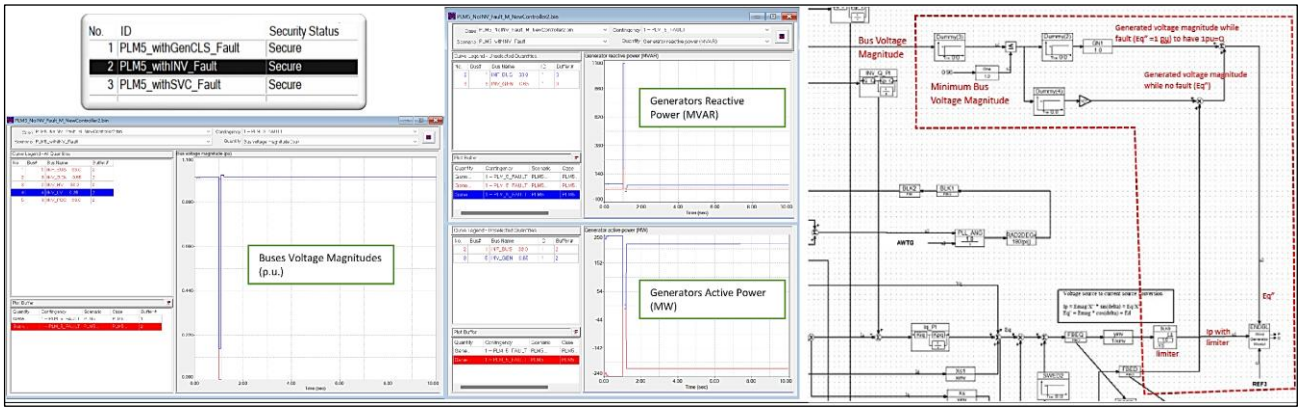
Newton-Raphson Solution

Iteration	Largest Mismatch	At Bus	Unsolved Buses	Sum of all Buses
1				
P Mismatch (MW)	0.00	2 INV_HV 33.0)	0	0.0
Angle Change (Rad)	0.000001	2 INV_HV 33.0)	0	0.0000
Q Mismatch (MVAr)	-0.01	4 INV_LV 0.65)	0	0.0
Voltage Change(pu)	-0.000001	4 INV_LV 0.65)	0	0.0000
2				
P Mismatch (MW)	-0.00	4 INV_LV 0.65)	0	0.0
Q Mismatch (MVAr)	-0.00	4 INV_LV 0.65)	0	0.0

Solution is reached in 2 iterations

Bus Number	Name	Base kV	Type	Voltage kV	PU	Angle	Fault Magnitude LLL	LLG	LL	LG	Area Number	Name	Zone Number	Name	Owner Number	Name
1	INF_BUS	33.0	33 Swing Bus	33.03	1.0009	0.0000	0	0	0	0	1	AREA 1	1	ZONE-001	1	Owner1
2	INV_HV	33.0	33 Load Bus	33.00	1.0000	11.7396	0	0	0	0	1	AREA 1	1	ZONE-001	1	Owner1
3	INV_POC	33.0	33 Load Bus	33.00	1.0000	11.7396	0	0	0	0	1	AREA 1	1	ZONE-001	1	Owner1
4	INV_LV	0.65	0.65 Load Bus	0.65	1.0005	13.3939	0	0	0	0	1	AREA 1	1	ZONE-001	1	Owner1
5	INV_GEN	0.65	0.65 Gen. Bus	0.65	1.0005	13.3939	0	0	0	0	1	AREA 1	1	ZONE-001	1	Owner1

(a)



(b)

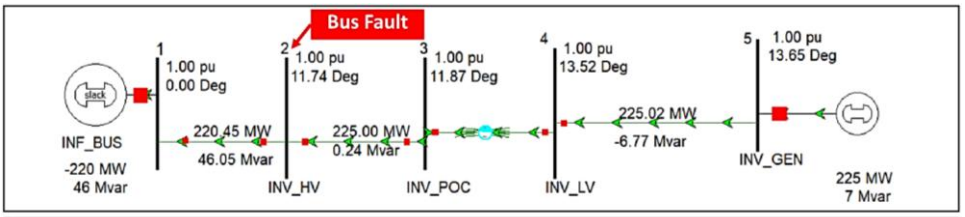
Figure A3.2. Results of the modified GFM model with improved fault-related behaviour in (a) PSAT and (b) TSAT.

Table A3.1. Comparison of the original and modified GFM models in DSATools.

Model version	PSAT result	TSAT result	SSAT SMIB result	Main remark
Original GFM model	Desirable	Limited / early-stage implementation	Desirable	Baseline SMIB representation used for the first GFM benchmark studies
Modified GFM model	Desirable	Improved, with fault-related / low-voltage capability	Desirable	Refined model with more suitable transient behaviour for later analytical studies

A.4 SMIB PowerWorld Analysis of Inertia and System Strength

This stage is the first systematic analytical study of GFM behaviour. It uses PowerWorld to investigate the effect of virtual inertia and line impedance on eigenvalues, damping ratio, and oscillation frequency in an SMIB system based on REGFM_B1. The main result was that both inertia and system strength materially influence oscillatory behaviour: increasing virtual inertia at fixed line reactance reduced both the natural frequency and damping ratio of the reported mode, while reducing line reactance at fixed H increased natural frequency and reduced damping ratio in the cases shown in Figure A4.4.



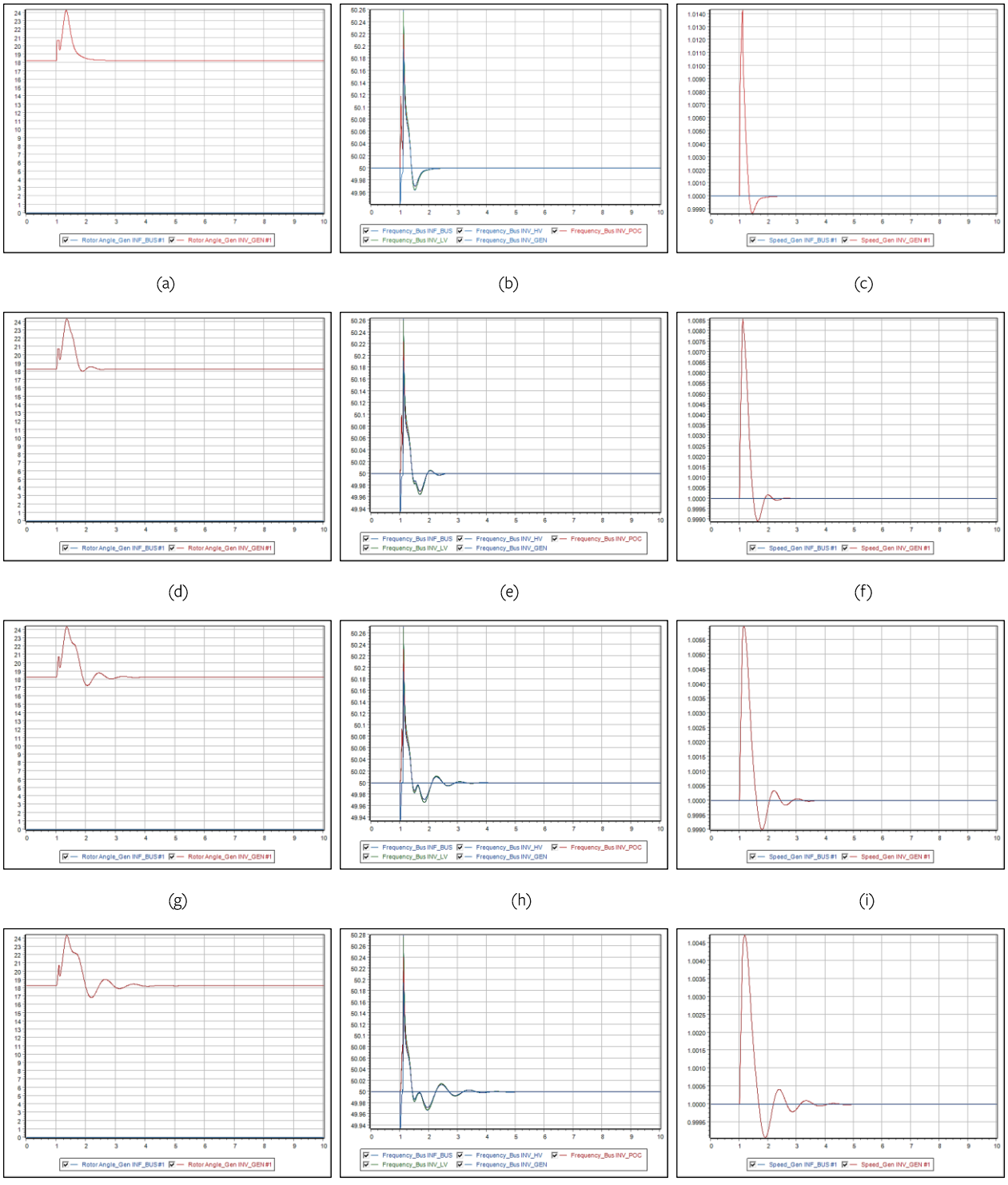
	Object Pretty	Time (Cycles)	Time (Seconds)	Enabled	Object	Description	Model Cr
1	Bus INV_HV	50.0	1.000000	CHECK	Bus '2'	FAULT 3PB SOLID SELFCLEAR	
2	Bus INV_HV	55.0	1.100000	CHECK	Bus '2'	CLEARFAULT	

(a)

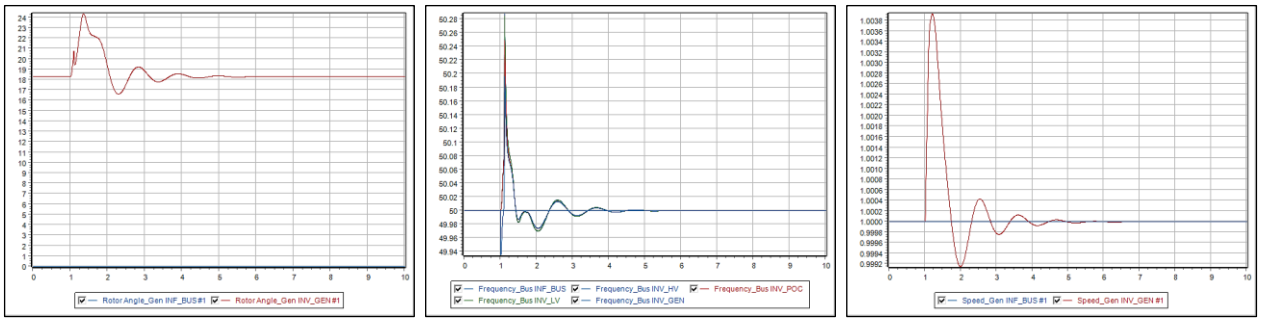
Bus Number	Name	Area Name	Nom kV	PU Volt	Volt (kV)	Angle (Deg)	Load MW	Load Mvar	Gen MW	Gen Mvar	Switched Shunts Mvar	Act G Shunt MW	Act B Shunt Mvar	Area Num	Zone Num	Bus Number
1	INF_BUS	AREA 1	33	1.0009	33.03	0			-220.45	46.05		0	0	1	1	1
2	INV_HV	AREA 1	33	1	33	11.74						0	0	1	1	2
3	INV_POC	AREA 1	33	1	33	11.87						0	0	1	1	3
4	INV_LV	AREA 1	0.65	1.00053	0.65	13.52						0	0	1	1	4
5	INV_GEN	AREA 1	0.65	1.0006	0.65	13.65			225.02	7.28		0	0	1	1	5

(b)

Figure A4.1. SMIB simulation in PowerWorld Simulator: (a) test system including REGFM_B1; and (b) initial power-flow study using the Newton-Raphson method for line parameters R = 0 and X = 0.001, with GFM inertia H = 2.5.

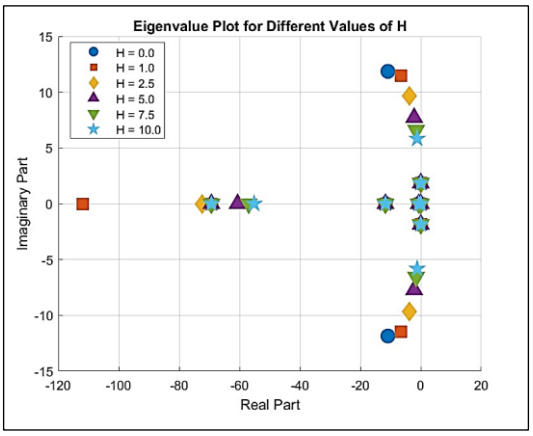


(j) (k) (l)

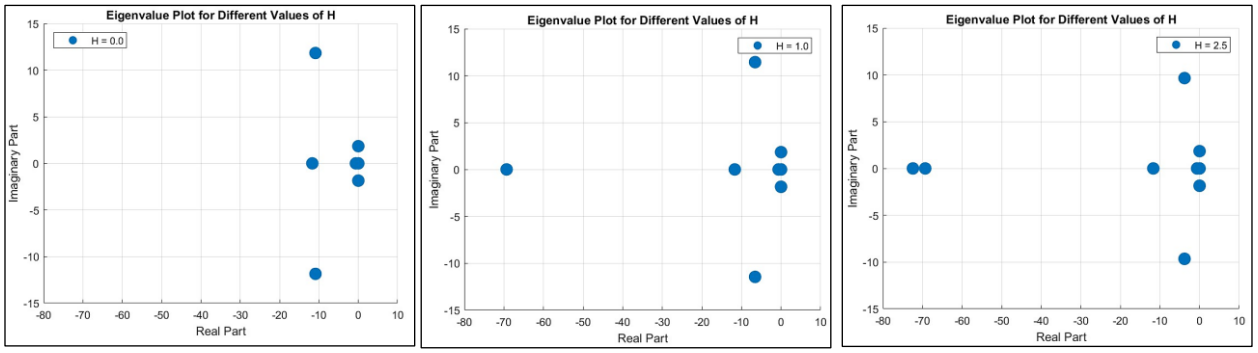


(m) (n) (o)

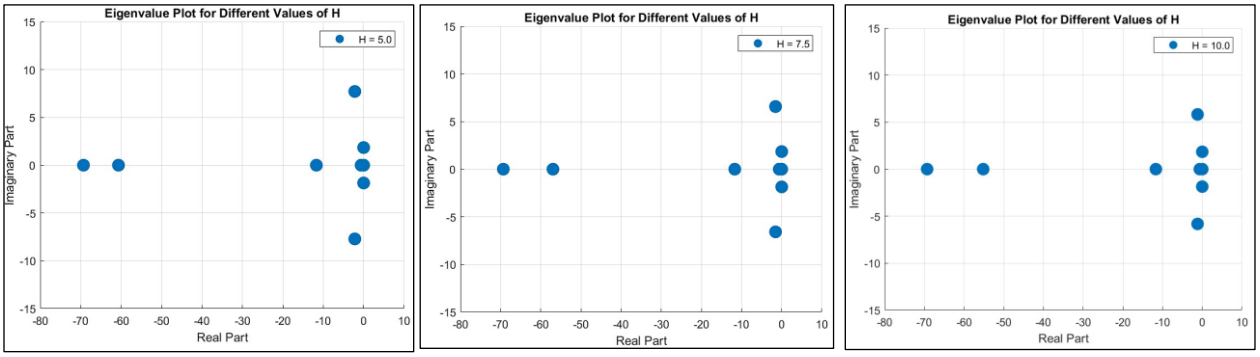
Figure A4.2. Transient-stability responses for increasing virtual inertia with line parameters $R = 0$ and $X = 0.001$: results for $H = 0$, (a) generator rotor angles, (b) bus frequencies, and (c) generator speeds; results for $H = 2.5$, (d) generator rotor angles, (e) bus frequencies, and (f) generator speeds; results for $H = 5$, (g) generator rotor angles, (h) bus frequencies, and (i) generator speeds; results for $H = 7.5$, (j) generator rotor angles, (k) bus frequencies, and (l) generator speeds; and results for $H = 10$, (m) generator rotor angles, (n) bus frequencies, and (o) generator speeds.



(a)



(b) (c) (d)



(e) (f) (g)

Figure A4.3. Effect of increasing REGFM_B1 virtual inertia on SMIB eigenvalues and oscillatory response: (a) all cases together; and individual cases for (b) H = 0, (c) H = 1, (d) H = 2.5, (e) H = 5, (f) H = 7.5, and (g) H = 10.

H	Dominant Eigenvalue	Damping Ratio ζ	Natural Frequency ωn
0	−10.9011±j11.9154j	0.6750	16.15
1	−6.5673±11.5041j	0.4958	13.25
2.5	−3.7993±9.695j	0.3649	10.41
5	−2.1866±7.7428j	0.2718	8.05
7.5	−1.5311±6.6031j	0.2259	6.78
10	−1.1782±5.8471j	0.1975	5.96

(a)

H	Dominant Eigenvalue	Damping Ratio ζ	Natural Frequency ωn
0	−10.7397±11.3606j	0.6870	15.63
1	−6.5018±11.0439j	0.5073	12.82
2.5	−3.7789±9.3416j	0.3750	10.08
5	−2.1818±7.4756j	0.2802	7.79
7.5	−1.5302±6.3802j	0.2332	6.56
10	−1.1789±5.652j	0.2042	5.77

(b)

H	Dominant Eigenvalue	Damping Ratio ζ	Natural Frequency ωn
0	−9.7937±7.1973j	0.8058	12.15
1	−6.1234±7.8153j	0.6168	9.93
2.5	−3.6659±6.9069j	0.4688	7.82
5	−2.1613±5.65j	0.3573	6.05
7.5	−1.5329±4.862j	0.3007	5.10
10	−1.1905±4.3253j	0.2654	4.49

(c)

Figure A4.4. Effect of virtual inertia and grid strength on oscillation damping ratio and frequency for different impedances of the line between Buses 2 and 3: (a) R=0 and X=0.001; (b) R=0 and X=0.01; and (c) R=0 and X=0.1.

Table A4.1. Summary of the observed effects of virtual inertia and line impedance in the SMIB study.

Variable changed	Observed effect on natural frequency	Observed effect on damping ratio	Interpretation
Increase virtual inertia H at fixed line reactance	Decreases over the reported H range	Decreases over the reported H range	Increasing H reduces both the natural frequency and damping ratio of the reported mode under the studied settings.
Decrease line reactance X at fixed H	Increases in the reported cases	Decreases in the reported cases	Lower line reactance does not imply a higher damping ratio for this mode under the studied settings.

The controller-parameter and network-reactance sweeps should be interpreted separately. Figure A4.4 shows that increasing H at fixed line reactance reduces both the natural frequency and damping ratio of the reported mode. At fixed H, reducing line reactance increases natural frequency but reduces damping ratio. Damping ratio and modal decay rate are distinct quantities; these results therefore do not support a general statement that strengthening the grid improves damping across the studied cases.

A.5 REGFM_B1 Validation in SMIB and Kundur Benchmark Systems

This stage marks a major increase in technical maturity. The project now moves beyond preliminary model exploration and demonstrates benchmark validation of REGFM_B1 using SMIB and Kundur systems, together with eigenvalue analysis, time-domain simulation, and matrix-pencil mode extraction. The main outcome was that the broad trends observed in the earlier SMIB studies were validated across multiple benchmark systems and analytical methods, thereby increasing confidence in the technical credibility of the later placement studies.

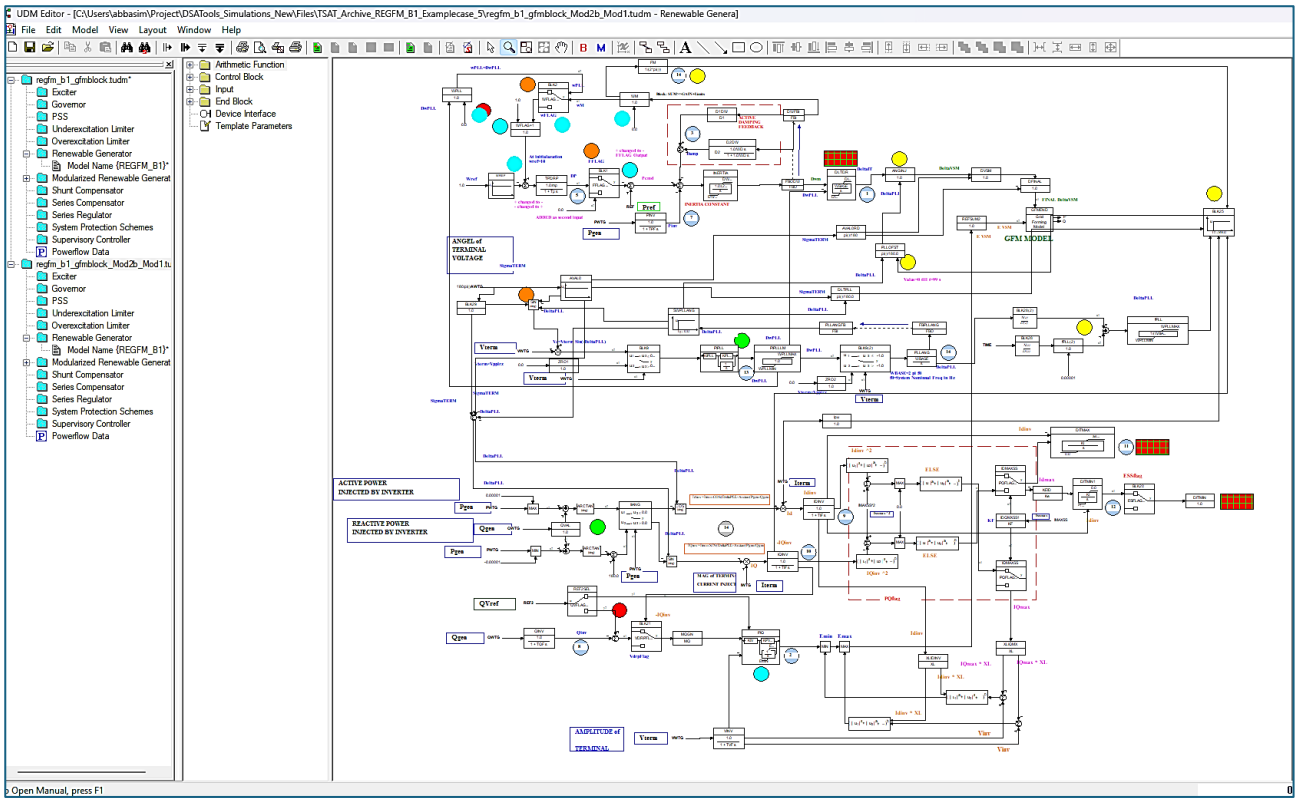
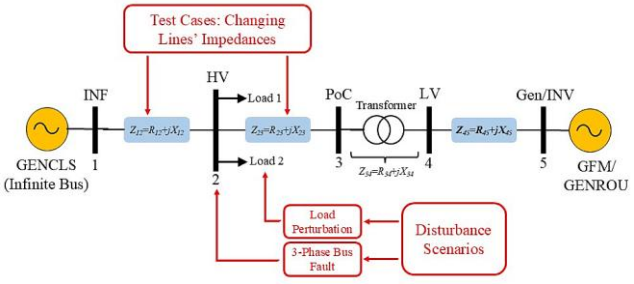
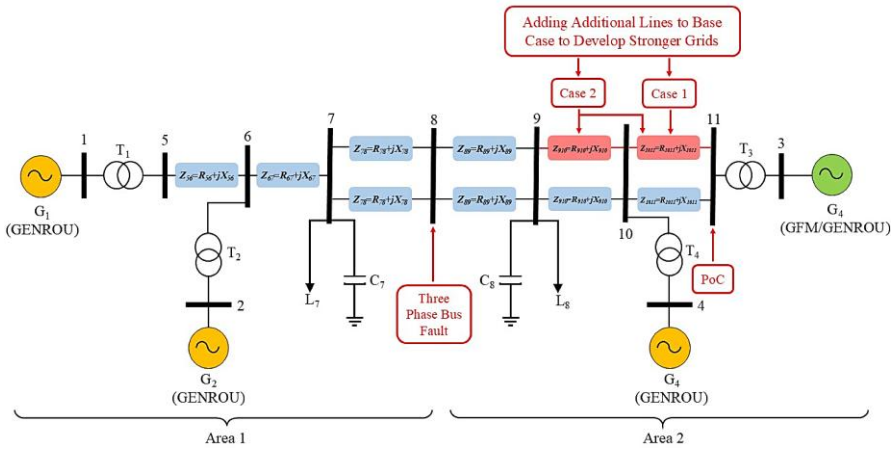


Figure A5.1. REGFM_B1 in the UDM Editor.



(a)



(b)

Figure A5.2. Single-line block diagrams of the benchmark test systems used in this stage of the study: (a) SMIB; and (b) Kundur.

Genrou at Bus 5: SMIB Eigenvalue Analysis PWS		
Grid Condition	**Frequency (Hz)**	**Damping Ratio (%)**
Case 1 (Base Case) $X_{12}=X_{23}=0.08$ **SCR=6.25**	1.155	13.1
Case 2 $X_{12}=X_{23}=0.1$ **SCR=5**	1.1115	13.53
Case 3 $X_{12}=X_{23}=0.3$ **SCR=1.67**	0.8175	18.84
Case 4 $X_{12}=X_{23}=0.5$ **SCR=1**	0.6257	23.92

(a)

GFM at Bus 5: SMIB Eigenvalue Analysis PWS		
Grid Condition	**Frequency (Hz)**	**Damping Ratio (%)**
Case 1 (Base Case) $X_{12}=X_{23}=0.08$ **SCR=6.25**	0.7758	38.26
Case 2 $X_{12}=X_{23}=0.1$ **SCR=5**	0.7328	40.65
Case 3 $X_{12}=X_{23}=0.3$ **SCR=1.67**	0.5112	61.41
Case 4 $X_{12}=X_{23}=0.5$ **SCR=1**	0.3926	81.78

(b)

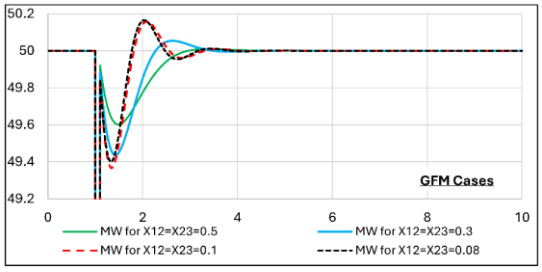
Genrou at Bus 5: Complete Eigenvalue Analysis SSAT		
Grid Condition	**Frequency (Hz)**	**Damping Ratio (%)**
Case 1 (Base Case) $X_{12}=X_{23}=0.08$ **SCR=6.25**	1.13	13.95
Case 2 $X_{12}=X_{23}=0.1$ **SCR=5**	1.0877	14.23
Case 3 $X_{12}=X_{23}=0.3$ **SCR=1.67**	0.8078	16.8
Case 4 $X_{12}=X_{23}=0.5$ **SCR=1**	0.6524	18.74

(c)

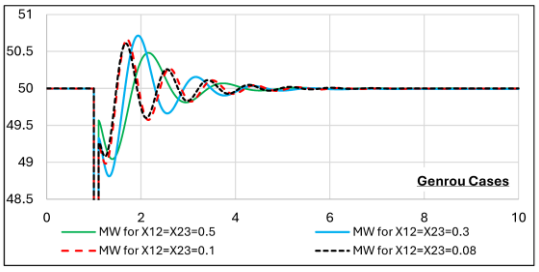
GFM at Bus 5: Complete Eigenvalue Analysis SSAT		
Grid Condition	**Frequency (Hz)**	**Damping Ratio (%)**
Case 1 (Base Case) $X_{12}=X_{23}=0.08$ **SCR=6.25**	0.8577	50.11
Case 2 $X_{12}=X_{23}=0.1$ **SCR=5**	0.7996	23.08
Case 3 $X_{12}=X_{23}=0.3$ **SCR=1.67**	0.417	77.83
Case 4 $X_{12}=X_{23}=0.5$ **SCR=1**	0.0556	99.44

(d)

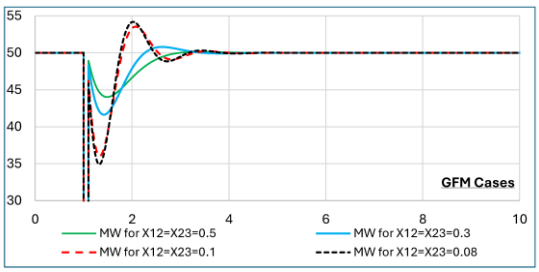
Figure A5.3. Eigenvalue comparison and benchmark validation of REGFM_B1 in PowerWorld Simulator (PWS) and the SSAT environment: (a) PWS eigenvalues for the SMIB case with GENROU; (b) PWS eigenvalues for the SMIB case with REGFM_B1; (c) SSAT eigenvalues for the complete system with GENROU; and (d) SSAT eigenvalues for the complete system with REGFM_B1.



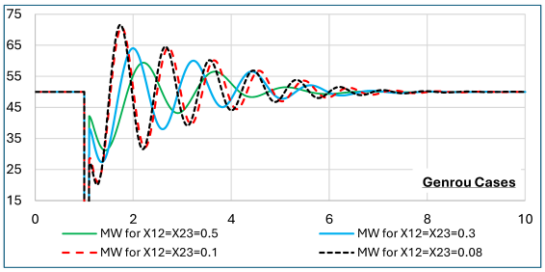
(a)



(b)

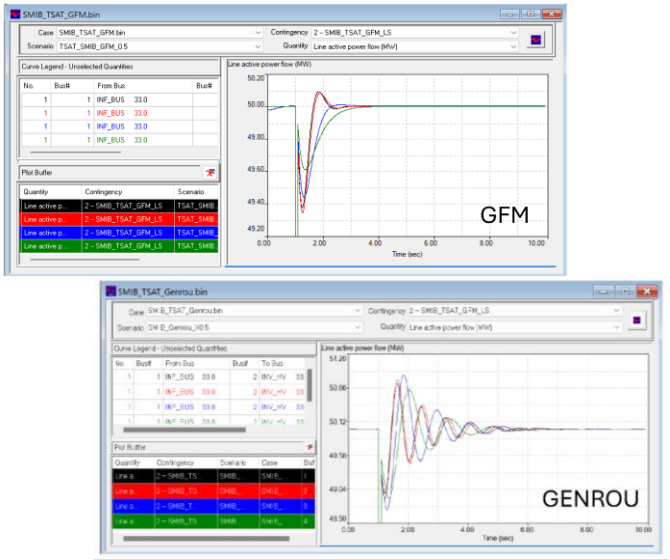


(c)

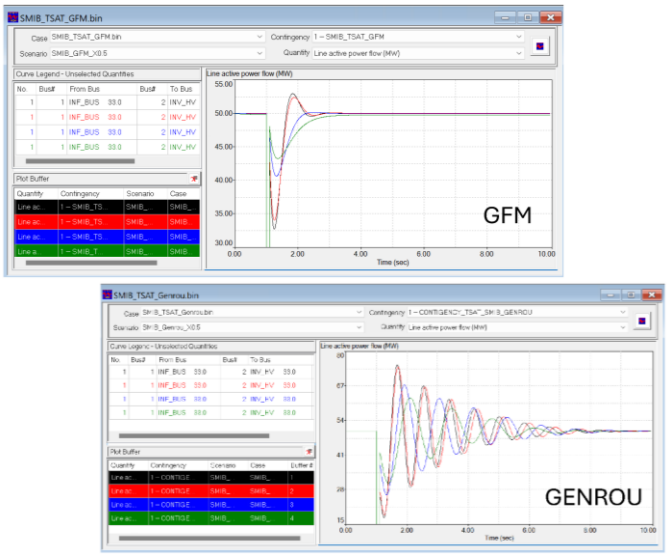


(d)

Figure A5.4. SMIB time-domain plots of active power (MW) in the PowerWorld Simulator environment: for a small disturbance (load perturbation of up to approximately 10%), (a) REGFM_B1 and (b) GENROU; and for a large disturbance (three-phase bolted fault, 5 cycles, self-clearing at PCC Bus 2), (c) REGFM_B1 and (d) GENROU.

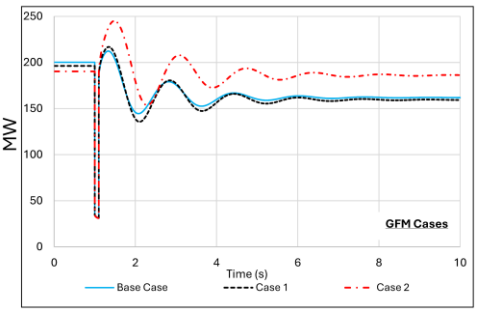


(a) (b)

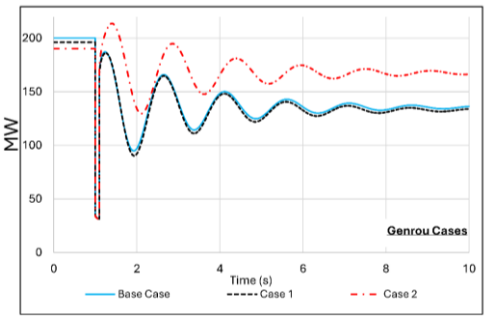


(c) (d)

Figure A5.5. SMIB time-domain plots in the TSAT environment: for a small disturbance (load perturbation of up to approximately 10%), (a) REGFM_B1 and (b) GENROU; and for a large disturbance (three-phase bolted fault, 5 cycles, self-clearing at PCC Bus 2), (c) REGFM_B1 and (d) GENROU.



(a)



(b)

Grid Type	Z_{10-11} pu	Z_{9-10}pu	$\lvert Z_{th}\rvert \angle$ angle (°) pu	SCR
Base Case	0.0025 + j0.025	0.001 + j0.01	0.2947 ∠ 85.91°	3.39
Case 1	0.00125 + j0.0125	0.0010 + j0.01	0.2821 ∠ 85.98°	3.54
Case 2	0.00125 + j0.0125	0.0005 + j0.005	0.2774 ∠ 86.01°	3.61

(c)

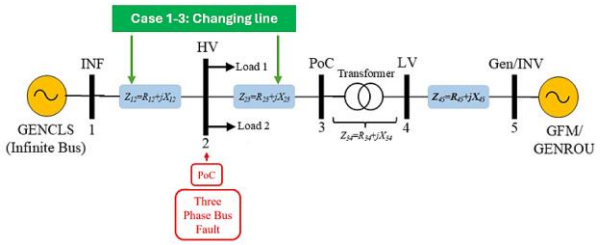
Figure A5.6. Kundur-system time-domain plots of active power (MW) in the PowerWorld Simulator environment for a large disturbance (three-phase fault at Bus 8, 5 cycles, self-clearing): (a) REGFM_B1; (b) GENROU; and (c) different parameter cases.

Table A5.1. Summary of benchmark-system validation results from June 2025.

System	Analysis type	Main variable examined	Main observation	Implication
SMIB	Time-domain simulation	Disturbance response under different grid-strength conditions	REGFM_B1 showed acceptable dynamic behaviour and contributed damping support	The GFM model was suitable for transient analysis in a benchmark setting
SMIB	Eigenvalue analysis	Modal characteristics under varying system strength	Damping and frequency changed with grid strength, confirming the importance of SCR and line conditions	GFM behaviour must be interpreted together with the surrounding network
SMIB	Matrix-pencil mode estimation	Oscillatory mode extraction	Modal estimates were consistent with the broad eigenvalue trends obtained from the benchmark studies	Independent modal estimation strengthened confidence in the observed results
Kundur two-area system	Time-domain and modal analysis	Inter-area mode behaviour	The GFM model provided damping support in a standard multi-machine benchmark system	The project findings were not limited to SMIB behaviour alone
Kundur two-area system	Comparative validation	Behaviour across benchmark systems	Broad trends observed in SMIB were also meaningful in the larger benchmark system	The validation stage justified moving to more advanced multiple-GFM placement studies

A.6 Tuning, Equivalence, and Multiple-GFM Interaction Studies

This stage is conceptually important because it addresses three deeper technical questions: how GFM and synchronous-machine behaviour can be approximately matched, how inertia and damping parameters affect dynamic response, and how multiple GFMs interact in the Kundur system. The main results were that approximate equivalence can be achieved only under selected conditions, that the main damping term has a stronger stabilising influence than virtual inertia alone, and that multiple GFMs are most effective when they are placed so as to participate strongly and appropriately in the oscillatory structure of the system.

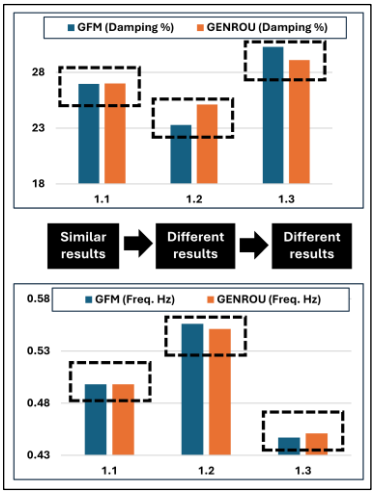


(a)

GENROU			
Case	Time Domain Plot	Parameter	Value (Inter-area mode)
1.1	MW Plot (Bus 1 and 2)	f, ζ	0.496 Hz, 27.11 %
1.2	MW Plot (Bus 1 and 2)	f, ζ	0.551 Hz, 25.12 %
1.3	MW Plot (Bus 1 and 2))	f, ζ	0.451 Hz, 29.10 %

GFM			
Case	Time Domain Plot	Parameter	Value (Inter-area mode)
1.1	MW Plot (Bus 1 and 2)	f, ζ	0.498 Hz, 26.96 %
1.2	MW Plot (Bus 1 and 2)	f, ζ	0.556 Hz, 23.28 %
1.3	MW Plot (Bus 1 and 2)	f, ζ	0.447 Hz, 30.29 %

(b)

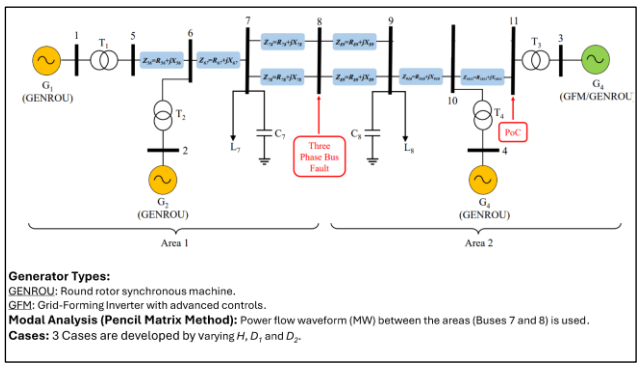


(c)

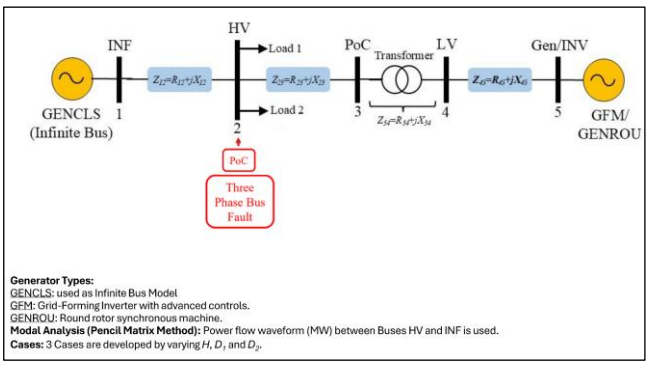
Figure A6.1. (a) SMIB test system used for tuning extraction; and matched modal behaviour of GENROU and REGFM_B1 shown as (b) numerical results and (c) a bar chart.

Goal	GENROU Knobs	REGFM_B1 Knobs
Match inertia	H	H
Match mode freq *f*	K_a ↑→ f↑	X_e↑/D_2↑→ f↓
Match damping ratio ζ	$PSS\ K_T$ ↑→ ζ↑ $Gov\ D_t$ ↑→ ζ↑ D ↑→ ζ↑	D_1 ↑→ ζ↑ m_p ↑→ ζ↓
Align droop (steady-state Δf)	R (droop)	m_p
Align reactive / V response	K_a, $R_{comp/Xcomp}$	k_{pv}/k_{iv}, m_q, X_e/R_e
Limits / saturation	$V_{rmax/min}$, $V_{max/min}$, H_{lim}	I_{ssmax}, $I_{faultmax}$, D_w limits

Figure A6.2. Tuning approach for approximate equivalence between GENROU and REGFM_B1.

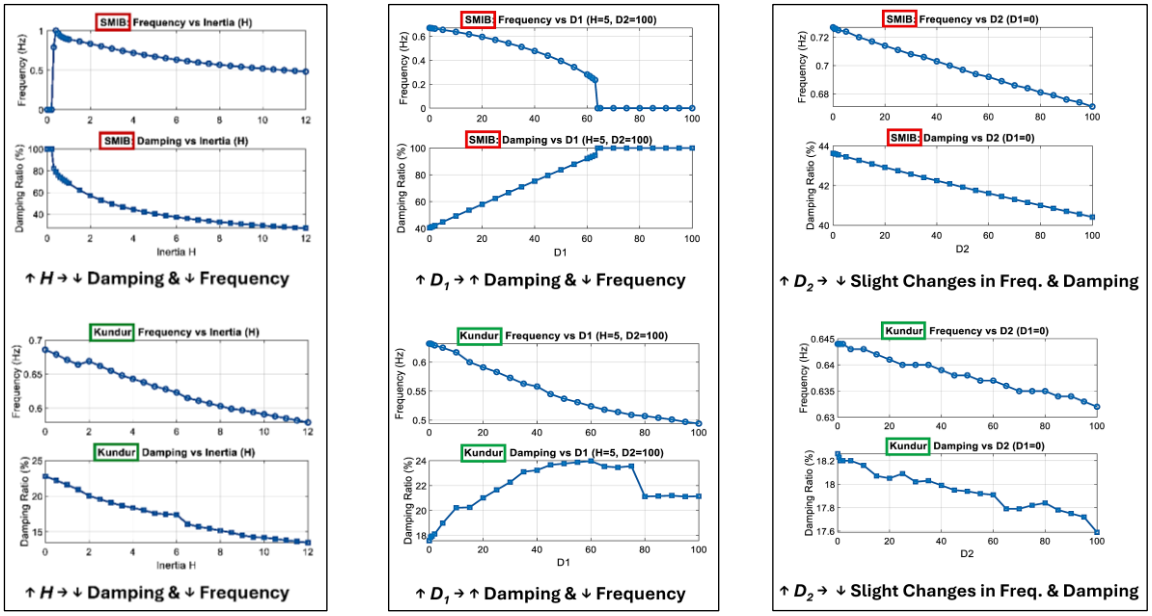


(a)



(b)

Figure A6.3. Test systems and case studies used to examine the impact of GFM parameters: (a) Kundur; and (b) SMIB.



(a) (b) (c)

Figure A6.4. Impact of H, D_1, and D_2 on GFM behaviour in the SMIB and Kundur systems: (a) varying inertia H (H = 0-12, D_1=0, D_2=100); (b) varying D_1 (H = 5, D_1=0-100, D_2=100); and (c) varying D_2 (H = 5, D_1=0, D_2=0-100).

Observations

- Similar behaviour can be obtained using the developed tuning recipe.
- Changing operating condition → Different Damping ratios
- Changing operating condition → Different Frequencies

Conclusion

- Changing operating condition → Different damping and frequency → Re-tuning is needed
- Further investigations are needed to develop a solution.

Figure A6.5. Summary of tuning-based equivalence and the effect of operating-condition changes on frequency and damping.

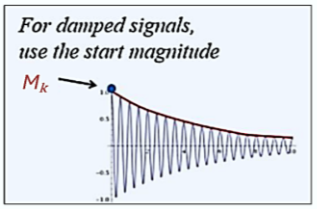
Any **transient signal** can be written as the sum of damped sinusoids (modes):

$$x(t) \approx \Sigma M_k e^{[\lambda_k (t-T_s)]} \cos(2\pi f_k (t-T_s) + \theta_k) \xrightarrow{t=T_s} x(t) \approx \Sigma M_k \cos(\theta_k)$$

Where:

- f_k = frequency (Hz)
- λ_k = exponential damping coefficient
- M_k = magnitude of the mode
- θ_k = phase angle

For damped signals, use the start magnitude



Damping ratio (as %):

$$\zeta_k (\%) = -100 \times \lambda_k / \sqrt{(\lambda_k^2 + (2\pi f_k)^2)}$$

Interpretation

- Larger M_k → stronger participation in mode
- Phase separation ~180° → opposing clusters (inter-area mode)
- Balanced magnitudes across areas → effective damping
- Non-GFM dominance → GFMs don't control oscillation

Figure A6.6. Modal-analysis equations and theoretical framework in PowerWorld Simulator.

Magnitude and phase patterns support interpretation of the observed responses; damping performance is assessed from the reported modal estimates. The magnitude-based participation measures describe contributions to the analysed signals.

Modal Analysis Results: Frequency & Damping for All Case

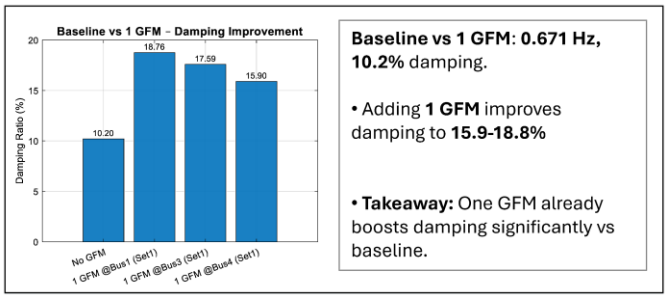
Scenario	Case	GFMs Bus	Placement	Parameter Set	Freq (Hz)	Damp (%)	Remark
No GFM	Baseline	N/A	N/A	N/A	0.671	10.2	Baseline
1 GFM	1.1	1	A1		0.666	18.8	**Improved**
	1.2	3	A2	Set 1	0.632	17.6	Improved
	1.3	4	A2		0.603	15.9	Improved
2 GFMs	2.1	1 & 3	Symmetric		0.637	29.0	Good
	2.2	1 & 4	Asymmetric	Set 1 & 1	0.630	26.8	Good
	2.3	3 & 4	Same Area		0.540	18.9	Poor
	3.1	1 & 3	Symmetric		0.718	**28.9**	**Good**
	3.2	1 & 4	Asymmetric	Set 1 & 2	0.691	25.8	Good
	3.3	3 & 4	Same Area		0.535	22.5	Weak
	4.1	1 & 3	Symmetric		0.587	**40.9**	BEST
	4.2	1 & 4	Asymmetric	Set 1 & 3	0.582	38.0	Very Good
	4.3	3 & 4	Same Area		0.505	**18.6**	WORST
	5.1	1 & 3	Symmetric		**0.693**	**36.8**	**Very Good**
	5.2	1 & 4	Asymmetric	Set 2 & 3	0.729	32.5	Good
	5.3	3 & 4	Same Area		0.499	20.4	Poor

Parameter set for GFMS:

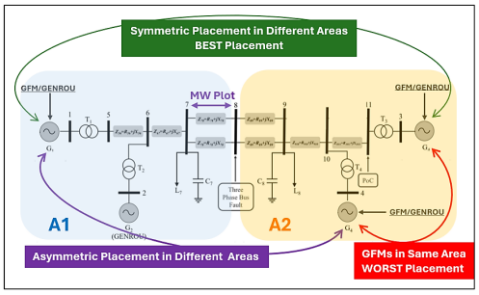
- **Set 1** (H=5, D1=0, D2=100)
- **Set 2** (**H=1**, D1=0, D2=100)
- **Set 3** (H=5, **D1=40**, D2=100)

Note: The cases include 0 to 2 GFMs in Kundur system with different or similar (like "Set 1 & 1") of parameters

(a)



(b)



(c)

Figure A6.7. Various GFM placements in the Kundur system: (a) outcomes for 0-2 GFM placements; (b) comparison of 0- and 1-GFM placement outcomes; and (c) visual summary of GFM placement effects.

Modal Analysis Results

Case	Placement	Gen.	Role	Area	Mag.	Angle (deg)	Freq. (Hz)	Damp. (%)
1.1	Symmetric	Bus 1	GFM	A1	**8.26**	**−42.46**	**0.639**	**28.86** BEST
		Bus 3	GFM	A2	**7.44**	**140.37**		
		Bus 2	GENROU	A1	7.31	−25.88		
		Bus 4	GENROU	A2	6.73	148.79		
1.2	Asymmetric	Bus 1	GFM	A1	**8.51**	**−54.63**	**0.630**	**26.37**
		Bus 4	**GFM**	A2	**7.13**	**125.95**		
		Bus 2	GENROU	A1	7.48	−36.75		
		Bus 3	GENROU	A2	8.00	135.05		
1.3	same-area	Bus 3	GFM	A2	**4.59**	**−95.16**	**0.542**	**18.55** WORST
		Bus 4	**GFM**	A2	**3.70**	**−95.65**		
		Bus 1	GENROU	A1	4.58	78.71		
		Bus 2	GENROU	A1	3.59	88.50		

(a)

Quantitative metrics derived from the modal analysis results

Case	GFM phase separation (°)	Area mean separation (°)	GFM balance = $\frac{min(M_{GFM1}, M_{GFM2})}{max(M_{GFM1}, M_{GFM2})}$	GFM share (%) = $100 \times \frac{M_{GFM1} + M_{GFM2}}{\sum_{g \in All} M_g}$
1.1	**177.17**	**178.75**	**0.901**	**52.79**
1.2	179.42	176.19	0.838	50.25
1.3	0.49	179.01	0.806	50.36

(b)

Figure A6.8. Two GFMs with identical parameters (H = 5, D_1=0, D_2=100) in the Kundur system: (a) modal-analysis results; and (b) quantitative metrics derived from the modal-analysis results.

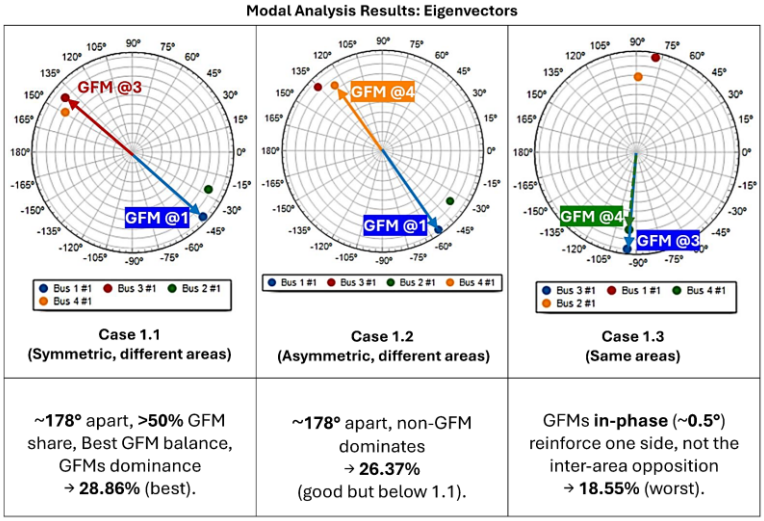


Figure A6.9. Placement outcomes in the Kundur system for two GFMs with identical parameters (H = 5, D_1=0, D_2=100).

Table A6.1. Summary of parameter-sensitivity and GFM-placement results from the September 2025 studies.

Case or parameter	Approximate effect on damping	Approximate effect on frequency	Interpretation
Increase (H)	Decreases	Decreases	Higher virtual inertia slows the response but can reduce damping if not coordinated with damping-related terms
Increase (D_1)	Generally increases; non-monotonic in the Kundur sweep	Decreases	(D_1) was the most effective stabilising parameter among those examined
Increase (D_2)	Small change	Small change	(D_2) had a comparatively weaker influence on modal behaviour
Baseline Kundur case	About 10.2% damping	About 0.671 Hz	Reference inter-area mode without GFM support
One GFM added	About 15.9–18.8% damping	About 0.603–0.666 Hz	A single GFM improves damping, but the result depends on location and parameter set
Best two-GFM case	About 40.9% damping	About 0.587 Hz	Symmetric cross-area placement with favourable damping support produced the best outcome
Weak same-area two-GFM case	About 18.6% damping	About 0.505 Hz	Concentrating both GFMs in one area was much less effective than balanced cross-area placement

A.7 Multiple-GFM Placement Analysis in the Simplified 14-Generator NEM Model

This stage examines how GFM placement affects inter-area oscillations in the simplified 14-generator NEM model. The subsection first presents the three-phase fault case at Bus 216, including representative best-versus-worst one- and two-GFM placements with H = 5, D_1 = 0, and D_2 = 100.

Table A7.1 presents a separate study using a small load-change disturbance at Bus 216, with $H = 5$, $D_1 = 20$, and $D_2 = 100$. The load-change disturbance was selected to help identify the oscillatory modes more clearly. These studies were conducted at different stages of the project to examine how frequency and damping change with GFM placement and number within each study set. The separate study sets were not intended for direct numerical comparison with each other. At $K = 0$, no GFM is present; therefore, the difference between the no-GFM baselines of the two Bus 216 studies is not attributable to D_1.

The subsection then presents the Bus 410 fault case and a summary of representative placement outcomes. The results show that placement matters, rather than device count alone. Favourable placements improve damping, but improvement is not guaranteed.

The frequencies, damping ratios, and associated complex modal poles in this subsection were estimated from simulation responses using the Matrix Pencil method. The disturbance itself does not change the eigenvalues of a fixed linearised model; rather, different disturbances can excite different modal components in the response, and the extracted estimates are sensitive to the selected analysis window. Within each analysed scenario, the identified inter-area modes are numbered from highest to lowest estimated frequency: Mode 1 has the highest frequency, followed by Mode 2 and Mode 3. These labels are scenario-specific and are not used to track a fixed physical mode across different GFM placements or disturbance cases. The polar plots show estimated mode shapes derived from the magnitudes and phases of the analysed signals.

For both the Bus 216 and Bus 410 fault cases, the fault is cleared without tripping any transmission line. Line connectivity therefore remains unchanged by fault clearing. For the Bus 216 case, the three-phase fault is applied at t = 1 s and cleared at t = 1.1 s.

Table A7.2 summarises representative results from the Bus 216 three-phase fault study with H = 5, D1 = 0, and D2 = 100.

	Case 1	Case 2	Case 3	Case 4	Case 5	Case 6
Load Condition	Heavy	Medium-heavy	Peak	Light	Medium	Light
Total generation (MW)	23030	21590	25430	15050	19060	14840
Total load (MW)	22300	21000	24800	14810	18600	14630
Inter-area flows	(North to south)	(South to north)	(Hydro to N & S)	(Area 2 to N & S)	(N & S to pumping)	(~Zero transfers)
Area 4 to Area 2 (MW)	500	-500	-500	-200	300	0
Area 2 to Area 1 (MW)	1134	-1120	-1525	470	740	270
Area 1 to Area 3 (MW)	1000	-1000	1000	200	-200	0
Area 3 to Area 5 (MW)	500	-500	250	200	250	0

Figure A7.1. Normal steady-state operating conditions of available versions of the simplified 14-generator Australian/NEM system based on the report by Gibbard and Vowles in [1].

Report: Inter-area modes (All PSS in service)

Case	Mode	Damped freq. Hz	Damping ratio (%)
1 H	11	0.579323993	27.56975771
	12	0.382290173	15.82630473
	13	0.286160588	27.88101949
2 M-H	11	0.562931034	21.24525838
	12	0.404571865	17.31885306
	13	0.279953545	23.79856707
3 P	11	0.589987374	28.89822635
	12	0.384836652	17.42964036
	13	0.296028194	29.76904425
4 L	11	0.776835277	21.6040788
	12	0.528712721	16.70935604
	13	0.399956372	22.81970612
5 M	11	0.621022588	22.0951258
	12	0.459798631	15.62434709
	13	0.311466224	24.61464611
6 Ls	11	0.739115556	22.61154908
	12	0.524893002	16.8855978
	13	0.390088766	20.7538929

SSAT: Inter-area modes (All PSS in service)

Case	Mode	Damped freq. Hz	Damping ratio (%)
1 H	11	0.579	27.49
	12	0.3822	15.6
	13	0.286	27.77
2 M-H	11	0.5629	21.27
	12	0.4053	17.24
	13	0.2803	23.6
3 P	11	0.5898	28.9
	12	0.385	17.48
	13	0.2962	29.8
4 L	11	0.7295	22.9
	12	0.5286	16.69
	13	0.4	22.79
5 M	11	0.6212	22.06
	12	0.4599	15.51
	13	0.3116	24.49
6 Ls	11	0.7394	22.57
	12	0.5244	16.87
	13	0.3901	20.69

PWS (Modal Analysis with 10% load change at Bus 216): Inter-area modes (All PSS in service)

Case	Mode	Plots: All_Gens_Rotor Angle		All_Gens_Speed		All_Gens_MW	
		Damped freq. Hz	Damping ratio (%)	Damped freq. Hz	Damping ratio (%)	Damped freq. Hz	Damping ratio (%)
1 H	1	0.529	27.585	0.564	26.922	0.581	29.028
	2	0.378	14.824	0.379	15.423	0.38	15.324
	3	0.276	25.12	0.286	25.78	0.285	28.606
2 M-H	1	0.553	20.234	0.557	19.854	0.55	21.26
	2	0.402	16.097	0.4	16.924	0.405	17.218
	3	0.276	22.042	0.275	24.789	0.274	27.488
3 P	1	0.577	25.596	0.565	31.346	0.587	28.109
	2	0.389	15.242	0.388	16.724	0.387	16.451
	3	0.314	29.808				
4 L	1	0.723	24.717	0.946	30.319	0.507	18.852
	2	0.526	15.223	0.574	33.228		
	3			0.518	19.79		
5 M	1	0.606	21.43	0.835	36.452	0.614	20.932
	2	0.456	14.052	0.451	16.157	0.456	14.849
	3	0.302	23.052	0.402	32.345	0.311	23.715
6 Ls	1	0.737	24.609	0.788	29.456	0.716	22.157
	2	0.518	15.76	0.518	15.674	0.518	15.558
	3	0.361	48.724				
	4	0.155	76.069				

Best Test System:

Case 1 has the most comparable inter-area results under small disturbance. Hence, inter-area modes can be detected better in this case.

Figure A7.2. Selection of test-system versions of the simplified 14-generator Australian/NEM system reported by Gibbard and Vowles [1], comparing the results from their report, SSAT, and PowerWorld Simulator (PWS).

The system is analyzed under progressive GFM deployment to assess the influence of inverter placement and penetration on system stability.

3-phase fault is applied to Bus 216 at t=1s and cleared at t=1.1s.

8 candidate units to replace with **REGFM_B1** (**4 in QLD + 4 in NSW**).

Scenario set (by K = # of REGFM_B1 installed)

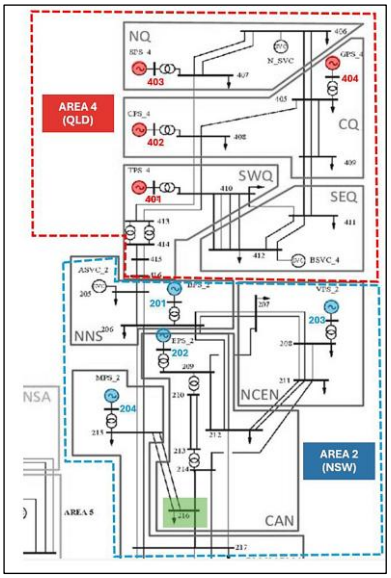
"Scenario **0…8**" below refers to the group with exactly **K** REGFM_B1 units.

Within each K, the number of distinct **cases** is **C(8, K)**. **Total scenarios across K=0…8 = 2^8 = 256** (includes baseline).

Hence, automating the simulations is a must.

K (Scenario label)	Meaning	# cases = C(8, K)	Cumulative cases (≤K)
0 (REGFM_B1 = 0)	Baseline: no replacements	1	1
1	Any 1 of the 8 candidates	8	9
2	Any 2 of the 8	28	37
3	Any 3 of the 8	56	93
4	Any 4 of the 8	70	163
5	Any 5 of the 8	56	219
6	Any 6 of the 8	28	247
7	Any 7 of the 8	8	255
8	All 8 replaced	1	256

(a)



(b)

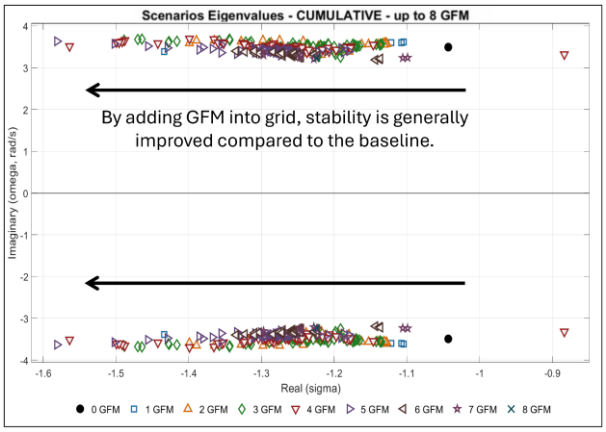
Figure A7.3. (a) GFM placement scenarios and explanatory notes used for the simplified 14-generator Australian/NEM system; and (b) Areas 4 and 2 of the simplified 14-generator Australian/NEM system, showing candidate GFM placement locations.

K	RankKind	Mode	ScenarioID including GFM placments	Frequency	Damping %	Eigen (*Real*)	Eigen (|*Im*|)
0	NA	1	S00_BASELINE_A42	0.555801	28.62572	-1.04333	3.492201
1	Worst	1	S_K=1_402_A42	0.575779	29.2077	-1.10483	3.617726
	Best	1	S_K=1_201_A42	0.539356	38.96222	-1.43368	3.388874
2	Worst	1	S_K=2_401-402_A42	0.573727	29.90885	-1.12988	3.604833
	Best	1	S_K=2_201-401_A42	0.5712	36.32419	-1.39923	3.588955
3	Worst	1	S_K=3_401-402-403_A42	0.567882	30.31362	-1.13503	3.568108
	Best	1	S_K=3_201-401-404_A42	0.582322	37.68958	-1.48879	3.658837
4	Worst	1	S_K=4_201-202-203-204_A42	0.528315	25.72837	-0.88381	3.319501
	Best	1	S_K=4_201-202-203-402_A42	0.559043	**40.67435**	-1.56393	3.512571
5	Worst	1	S_K=5_203-401-402-403-404_A42	0.552617	32.4337	-1.19052	3.472195
	Best	1	S_K=5_201-202-203-401-402_A42	0.578177	**39.90907**	-1.58119	3.632793
6	Worst	1	S_K=6_201-202-203-204-401-404_A42	0.512571	33.28048	-1.13662	3.220579
	Best	1	S_K=6_201-202-203-401-402-403_A42	0.540818	36.57069	-1.33518	3.39806
7	Worst	1	S_K=7_201-202-203-204-401-402-404_A42	0.515628	32.13005	-1.09923	3.239786
	Best	1	S_K=7_201-202-203-401-402-403-404_A42	0.525807	36.54835	-1.29721	3.303743
8	NA	1	S_K=8_201-202-203-204-401-402-403-404_A42	0.514146	35.43795	-1.22427	3.230475

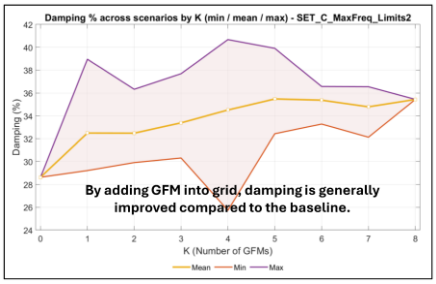
Figure A7.4. Best- and worst-case 0-8 GFM placements for Mode 1 in Areas 4 and 2 of the simplified 14-generator NEM model when the disturbance is applied to Bus 216; identical GFM parameters are used (H = 5, D_1=0, D_2=100).

K	RankKind	Mode	ScenarioID including GFM placments	Frequency	Damping %	Eigen (*Real*)	Eigen (|*Im*|)
0	NA	2	S00_BASELINE_A42	0.379551	14.29853332	-0.34453	2.384789
1	Worst	2	S_K=1_401_A42	0.377776	16.60827	-0.39977	2.373637
	Best	2	S_K=1_201_A42	0.363671	21.20132	-0.49572	2.285012
2	Worst	2	S_K=2_403-404_A42	0.366061	16.41974	-0.38286	2.300029
	Best	2	S_K=2_202-204_A42	0.357266	22.9396	-0.52905	2.244768
3	Worst	2	S_K=3_402-403-404_A42	0.365293	16.36378	-0.38071	2.295204
	Best	2	S_K=3_201-202-204_A42	0.34951	24.56245	-0.55645	2.196036
4	Worst	2	S_K=4_401-402-403-404_A42	0.365695	16.48906	-0.38413	2.297729
	Best	2	S_K=4_201-202-203-401_A42	0.3638	**26.39612**	-0.62556	2.285823
5	Worst	2	S_K=5_203-401-402-403-404_A42	0.360445	19.12072	-0.44117	2.264743
	Best	2	S_K=5_201-202-203-401-402_A42	0.350103	**26.09788**	-0.5947	2.199762
6	Worst	2	S_K=6_202-203-401-402-403-404_A42	0.355623	22.47174	-0.5153	2.234445
	Best	2	S_K=6_201-202-204-401-402-403_A42	0.343804	25.27199	-0.56424	2.160184
7	Worst	2	S_K=7_202-203-204-401-402-403-404_A42	0.347276	24.09353	-0.54168	2.181999
	Best	2	S_K=7_201-202-204-401-402-403-404_A42	0.342083	25.24761	-0.56083	2.149371
8	NA	2	S_K=8_201-202-203-204-401-402-403-404_A42	0.342316	25.15268	-0.55896	2.150835

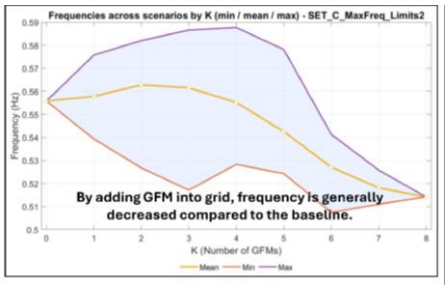
Figure A7.5. Best- and worst-case 0-8 GFM placements for Mode 2 in Areas 4 and 2 of the simplified 14-generator NEM model when the disturbance is applied to Bus 216; identical GFM parameters are used (H = 5, D_1=0, D_2=100).



(a)

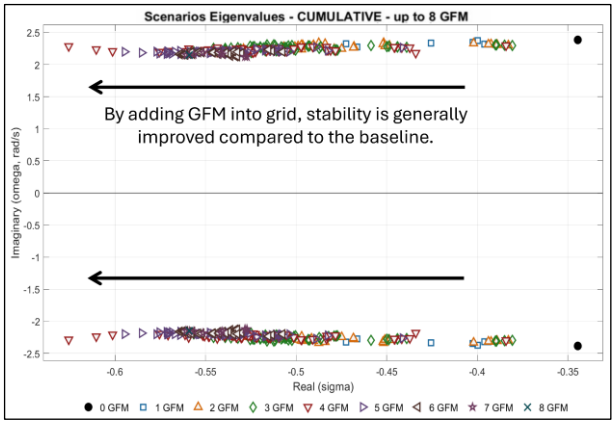


(b)

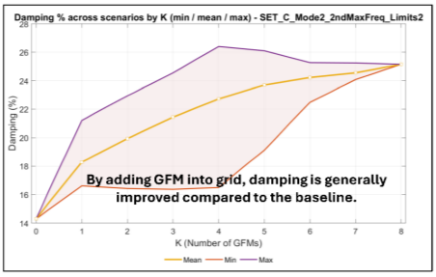


(c)

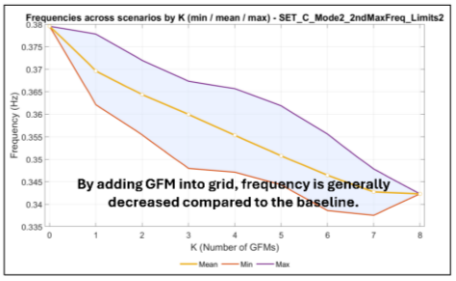
Figure A7.6. Inter-area oscillation study of 0-8 GFM placements for Mode 1 in the simplified 14-generator NEM model when the disturbance is applied to Bus 216; identical GFM parameters are used (H = 5, D_1=0, D_2=100): (a) scenario eigenvalues; (b) damping ratio across scenarios; and (c) frequency across scenarios.



(a)



(b)



(c)

Figure A7.7. Inter-area oscillation study of 0-8 GFM placements for Mode 2 in the simplified 14-generator NEM model when the disturbance is applied to Bus 216; identical GFM parameters are used (H = 5, D_1=0, D_2=100): (a) scenario eigenvalues; (b) damping ratio across scenarios; and (c) frequency across scenarios.

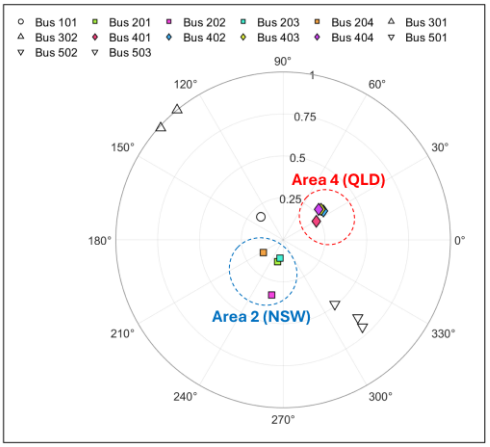
Results obtained for Baseline case (No GFM)

ScenarioID	Mode (inter-area)	Damping %	Frequency	Eigenvalue Real	Eigenvalue |Imag|
S00_BASELINE_A42	**1**	**28.62572189**	**0.555801**	**-1.04333**	**3.492201**

Inter-area modes by signal for Baseline (No GFM)

ScenarioID	BusNum	BusName	Mag.	Phase Angle	Area
S00_BASELINE_A42	**301**	**3_LPSGEN**	**29.80968**	**129.3127**	**3**
S00_BASELINE_A42	302	3_YPSGEN	29.49923	137.6804	3
S00_BASELINE_A42	501	5_NPSGEN	20.94413	-47.5528	5
S00_BASELINE_A42	503	5_PPSGEN	19.17623	-46.079	5
S00_BASELINE_A42	502	5_TPSGEN	14.67513	-51.1433	5
S00_BASELINE_A42	202	2_EPSGEN	9.968009	-101.729	2
S00_BASELINE_A42	402	4_CPSGEN	8.847879	35.51419	4
S00_BASELINE_A42	403	4_SPSGEN	8.692973	38.68855	4
S00_BASELINE_A42	404	4_GPSGEN	8.334042	40.70035	4
S00_BASELINE_A42	401	4_TPSGEN	6.759553	29.1417	4
S00_BASELINE_A42	101	1_HPSGEN	5.699728	134.0992	1
S00_BASELINE_A42	204	2_MPSGEN	4.160886	-147.438	2
S00_BASELINE_A42	201	2_BPSGEN	3.990084	-104.673	2
S00_BASELINE_A42	203	2_VPSGEN	3.285757	-99.6505	2

(a)

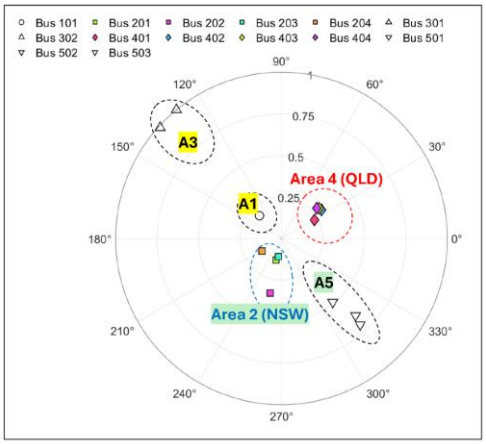


(b)

Figure A7.8. Baseline (no GFM) results for Mode 1 in the simplified 14-generator NEM model when the disturbance is applied to Bus 216: (a) inter-area modes, including modes identified by signal; and (b) eigenvector.

Area-based participation					
Area	Region	Generators	Sum of mags	Mode share	Area avg phase angle
A1	SH	101	5.70	3.3%	+134.1°
A2	NSW	201–204	21.40	12.3%	−110.4°
A3	VIC	301–302	59.31	34.1%	+133.5°
A4	QLD	401–404	32.63	18.8%	+36.4°
A5	SA	501–503	54.80	31.5%	−48.0°

Baseline pattern: dominant inter-area swing is essentially **[SH (A1) + VIC (A3)]** versus **[SA (A5)+ NSW (A2)]**, with **QLD (A4) acting as an intermediate/bridge area.**



(a) (b)

Figure A7.9. Baseline (no GFM) results for Mode 1 in the simplified 14-generator NEM model when the disturbance is applied to Bus 216: (a) area-based participation and interpretation; and (b) eigenvector.

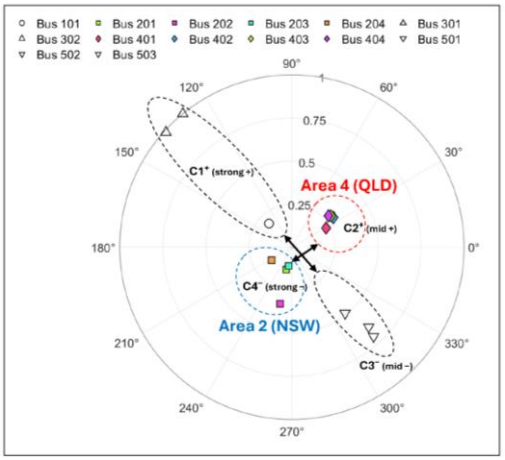
Phase angle-based clustering of generators				
Cluster	Mean angle	Members (buses)	Sum of mags	Mode share
C1 (VIC+SH)	+133.5°	301, 302, 101	65.01	37.4%
C2 (QLD)	+36.4°	401, 402, 403, 404	32.63	18.8%
C3 (SA)	−48.0°	501, 502, 503	54.80	31.5%
C4 (NSW)	−110.4°	201, 202, 203, 204	21.40	12.3%

Main opposing pair:

C1 (+133.5°) vs C3 (−48.0°)
Angle separation ≈ 181.5° → almost perfectly anti-phase.
Together they carry ≈ 69% of the mode → core inter-area oscillation.

Secondary opposing pair:

Despite acting on the "bridge/transition" side of the pattern, C2 and C4 are themselves strongly out of phase (≈150° separation).
C4 (−110.4°) is a more negative extension of the "− side", still opposing C1.
C2 (+36.4°) lies between C1 and C3, acting as a transition/bridge cluster.



(a) (b)

Figure A7.10. Baseline (no GFM) results for Mode 1 in the simplified 14-generator NEM model when the disturbance is applied to Bus 216: (a) phase-angle-based clustering of generators and interpretation; and (b) eigenvector.

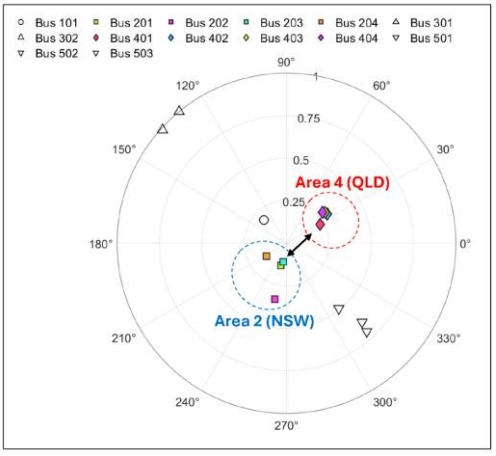
NSW–QLD Opposition (Generator Level)						
Side	Generators	Angle range (°)	Most opposite area	Typical Δθ to that area	Main opposite generator(s)	Typical Δθ to that gen
NSW (A2)	201, 202, 203	−105 to −100	QLD (A4)	−136–141°	404 (QLD)	−140–145°
NSW (A2)	204	−147	QLD (A4)	−176°	402 (QLD)	−177°
QLD (A4)	401–404	+29 to +41	NSW (A2)	−140–151°	204 (NSW)	−172–177°

Key points:

- For **every NSW generator (201–204)**, the **most opposite area** is **QLD (A4)**.
- For **every QLD generator (401–404)**, the **most opposite area** is **NSW (A2)**.
- **NSW 201–203**: strongest single opponent is **QLD 404** (≈140–145° away).
- **NSW 204**: almost perfectly anti-phase to **QLD 402** (≈177° separation).
- For **all QLD units**, the most opposite single generator is **NSW 204** (≈172–177°).

Interpretation:

- **NSW (A2)** and **QLD (A4)** form a **strong anti-phase pair** in this mode, with **NSW 204** and **QLD 402** sitting in the most **high-leverage opposite positions**.



(a) (b)

Figure A7.11. Baseline (no GFM) results for Mode 1 in the simplified 14-generator NEM model when the disturbance is applied to Bus 216: (a) NSW-QLD opposition at generator level and interpretation and key points; and (b) eigenvector.

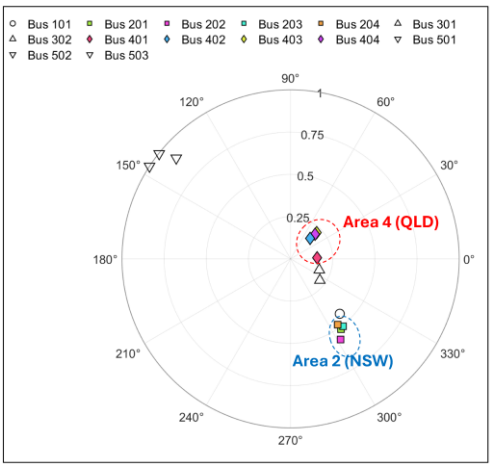
Results obtained for Baseline case (No GFM)

ScenarioID	Mode (inter-area)	Damping %	Frequency	Eigenvalue Real	Eigenvalue |Imag|
S00_BASELINE_A42	**2**	14.29853	0.379551	-0.34453	2.384789

Inter-area modes by signal for Baseline (No GFM)

ScenarioID	BusNum	BusName	Mag.	Phase Angle	Area
S00_BASELINE_A42	**501**	**5_NPSGEN**	**37.18934**	**146.7837**	**5**
S00_BASELINE_A42	503	5_PPSGEN	37.08478	141.4073	5
S00_BASELINE_A42	502	5_TPSGEN	33.5706	138.6787	5
S00_BASELINE_A42	202	2_EPSGEN	20.92576	-58.1403	2
S00_BASELINE_A42	201	2_BPSGEN	19.06256	-54.3252	2
S00_BASELINE_A42	203	2_VPSGEN	18.83234	-52.1544	2
S00_BASELINE_A42	204	2_MPSGEN	17.86235	-54.364	2
S00_BASELINE_A42	101	1_HPSGEN	16.23634	-48.0862	1
S00_BASELINE_A42	403	4_SPSGEN	8.168056	44.88845	4
S00_BASELINE_A42	302	3_YPSGEN	7.98938	-36.0962	3
S00_BASELINE_A42	404	4_GPSGEN	7.622603	45.26056	4
S00_BASELINE_A42	301	3_LPSGEN	6.780838	-20.9037	3
S00_BASELINE_A42	402	4_CPSGEN	6.269423	46.28473	4
S00_BASELINE_A42	401	4_TPSGEN	5.855847	2.163533	4

(a)



(b)

Figure A7.12. Baseline (no GFM) results for Mode 2 in the simplified 14-generator NEM model when the disturbance is applied to Bus 216: (a) inter-area modes, including modes identified by signal; and (b) eigenvector.

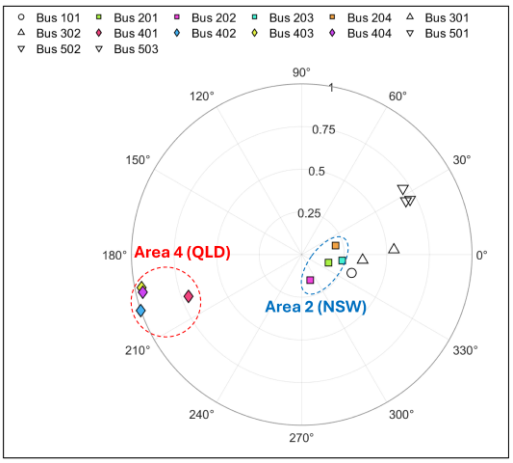
Results obtained for Baseline case (No GFM)

ScenarioID	Mode (inter-area)	Damping %	Frequency	Eigenvalue Real	Eigenvalue |Imag|
S00_BASELINE_A42	**3**	27.85333	0.265627	-0.48402	1.668984

Inter-area modes by signal for Baseline (No GFM)

ScenarioID	BusNum	BusName	Mag.	Phase Angle	Area
S00_BASELINE_A42	402	4_CPSGEN	17.81228	-160.839	**4**
S00_BASELINE_A42	403	4_SPSGEN	17.12232	-168.403	4
S00_BASELINE_A42	404	4_GPSGEN	17.09712	-166.729	4
S00_BASELINE_A42	502	5_TPSGEN	12.71219	26.91737	5
S00_BASELINE_A42	501	5_NPSGEN	12.64031	33.09992	5
S00_BASELINE_A42	401	4_TPSGEN	12.6098	-159.782	4
S00_BASELINE_A42	503	5_PPSGEN	12.26323	27.20883	5
S00_BASELINE_A42	301	3_LPSGEN	9.657774	2.945539	3
S00_BASELINE_A42	302	3_YPSGEN	6.398313	-5.17758	3
S00_BASELINE_A42	101	1_HPSGEN	5.562109	-20.1591	1
S00_BASELINE_A42	203	2_VPSGEN	4.262945	-8.54875	2
S00_BASELINE_A42	204	2_MPSGEN	3.648429	15.18103	2
S00_BASELINE_A42	201	2_BPSGEN	2.919539	-17.2466	2
S00_BASELINE_A42	202	2_EPSGEN	2.816838	-71.8703	2

(a)



(b)

Figure A7.13. Baseline (no GFM) results for Mode 3 in the simplified 14-generator NEM model when the disturbance is applied to Bus 216: (a) inter-area modes, including modes identified by signal; and (b) eigenvector.

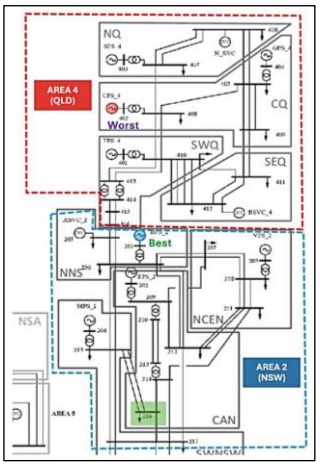
Inter-area mode for scenarios with 0-1 GFMs

K	RankKind	Mode	ScenarioID	Freq.	Damp %
0	NA	1	S00_BASELINE_A42	0.555801	28.62572
1	Best	1	S_K=1_201_A42	0.539356	38.96222
	2nd Best	1	S_K=1_202_A42	0.543056	35.39235
	-	1	S_K=1_203_A42	0.547028	32.42027
	-	1	S_K=1_204_A42	0.539496	34.85014
	2nd Worst	1	S_K=1_401_A42	0.573106	29.39877
	Worst	1	S_K=1_402_A42	0.575779	29.2077
	-	1	S_K=1_403_A42	0.572655	29.7685
	-	1	S_K=1_404_A42	0.572161	29.95655

Key summary:

- **Any GFM in NSW (A2)** → **clear damping improvement** (32–39%, all > baseline).
- **Any GFM in QLD (A4)** → damping only ~29–30% (slight improvement compared to baseline).

(a)

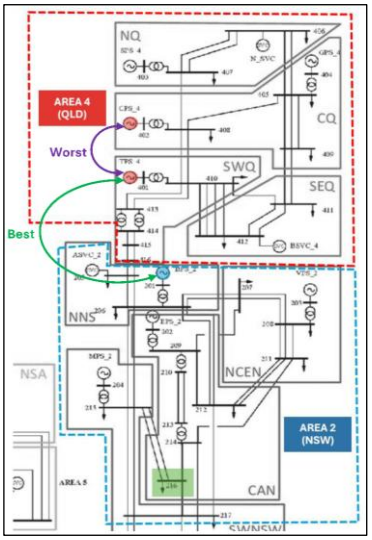


(b)

Figure A7.14. Results for zero- and one-GFM placements in the simplified 14-generator NEM model when the disturbance is applied to Bus 216; GFM parameters used are H = 5, D_1=0, D_2=100: (a) inter-area modes for all cases, with key summary; and (b) best and worst locations in Areas 2 and 4 of the system.

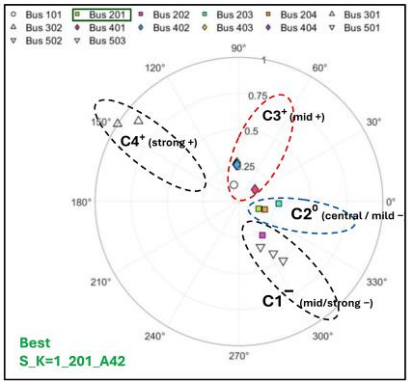
K	Rank	ScenarioID	Mode	Freq	Damping %
0	NA	S00_BASELINE_A42	1	0.555801	28.62572189
2	-	S_K=2_201-202_A42	1	0.538751	32.91373316
	-	S_K=2_201-203_A42	1	0.537267	33.34494618
	-	S_K=2_201-204_A42	1	0.542247	33.46959889
	Best	S_K=2_201-401_A42	1	0.5712	36.32419332
	-	S_K=2_201-402_A42	1	0.577633	34.36310087
	-	S_K=2_201-403_A42	1	0.581593	34.98804321
	-	S_K=2_201-404_A42	1	0.581197	35.56187208
	-	S_K=2_202-203_A42	1	0.535335	34.16052194
	-	S_K=2_202-204_A42	1	0.531963	34.75171045
	-	S_K=2_202-401_A42	1	0.573376	33.64111056
	-	S_K=2_202-402_A42	1	0.578471	32.35276478
	-	S_K=2_202-403_A42	1	0.581946	32.92884976
	-	S_K=2_202-404_A42	1	0.582067	33.44836565
	-	S_K=2_203-204_A42	1	0.526771	34.53303611
	-	S_K=2_203-401_A42	1	0.566289	30.51297854
	-	S_K=2_203-402_A42	1	0.569951	30.03654141
	-	S_K=2_203-403_A42	1	0.567185	30.77990239
	-	S_K=2_203-404_A42	1	0.566191	31.05751172
	-	S_K=2_204-401_A42	1	0.554785	31.82774075
	-	S_K=2_204-402_A42	1	0.558693	31.64500773
	-	S_K=2_204-403_A42	1	0.559609	32.82719263
	-	S_K=2_204-404_A42	1	0.559514	33.21201717
	Worst	S_K=2_401-402_A42	1	0.573727	29.90884681
	-	S_K=2_401-403_A42	1	0.57058	30.07147437
	-	S_K=2_401-404_A42	1	0.570249	30.14806679
	-	S_K=2_402-403_A42	1	0.568343	30.13565351
	-	S_K=2_402-404_A42	1	0.567999	30.21306704
	-	S_K=2_403-404_A42	1	0.565758	30.332299

(a)

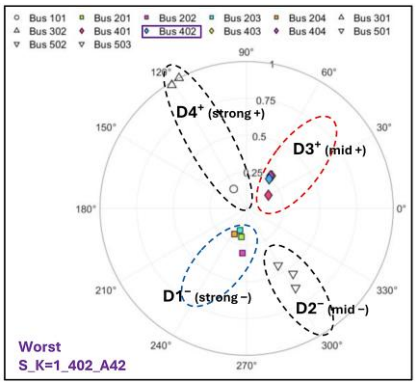


(b)

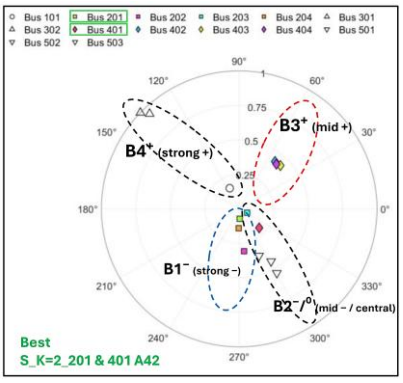
Figure A7.15. Results for zero- and two-GFM placements in the simplified 14-generator NEM model when the disturbance is applied to Bus 216; GFM parameters used are H = 5, D_1=0, D_2=100: (a) inter-area modes for all cases; and (b) best and worst locations in the system.



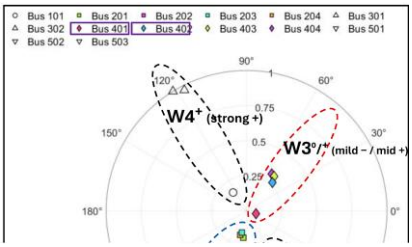
(a)



(b)



(c)



(d)

Figure A7.16. Angle-based clustering interpretation of representative best and worst one- and two-GFM placements in the simplified 14-generator NEM model for the Bus 216 disturbance case, with REGFM_B1 parameters H = 5, D_1 = 0, and D_2 = 100: (a) best K = 1 case (GFM

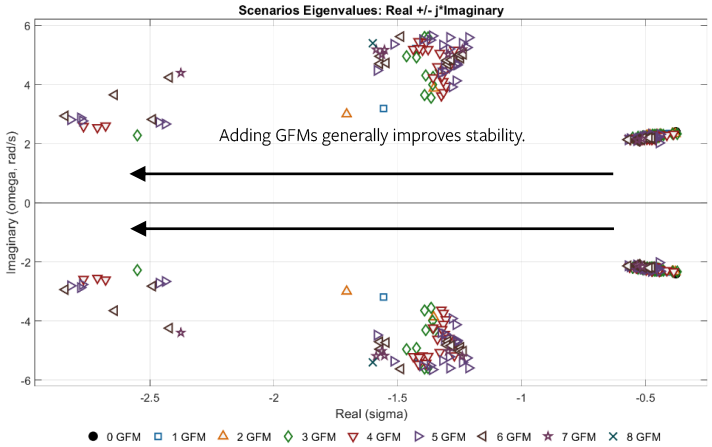
at Bus 201, NSW); (b) worst K = 1 case (GFM at Bus 402, QLD); (c) best K = 2 case (GFMs at Buses 201 and 401); and (d) worst K = 2 case (GFMs at Buses 401 and 402, QLD).

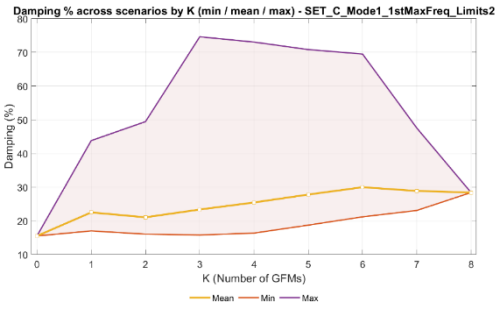
Table A7.1. Best- and worst-case 0-5 GFM placements for Mode 1 in the simplified 14-generator NEM model for the small load-change disturbance at Bus 216, with increased damping constant (D_1=20).

K	RankKind	Mode	ScenarioID including GFM placement	Frequency	Damping %	Eigen (Real)	Eigen ($\|I_m\|$)
0	NA	1	S00_BASELINE_A42	0.537494	29.33696	-1.03636	3.377174
1	Worst	1	S_K=1_404_A42	0.368324	16.77283	-0.39374	2.314248
	Best	1	S_K=1_201_A42	0.519784	50.00142	-1.88564	3.265899
2	Worst	1	S_K=2_403-404_A42	0.36596	16.54996	-0.38587	2.299394
	Best	1	S_K=2_201-204_A42	0.407498	50.71801	-1.50675	2.560385
3	Worst	1	S_K=3_402-403-404_A42	0.365258	16.53107	-0.38468	2.294984
	Best	1	S_K=3_201-401-402_A42	0.328119	64.65466	-1.74726	2.061632
4	Worst	1	S_K=4_401-402-403-404_A42	0.365951	16.86356	-0.39338	2.299338
	Best	1	S_K=4_201-202-402-404_A42	0.227016	82.49322	-2.08175	1.426384
5	Worst	1	S_K=5_203-204-402-403-404_A42	0.343377	19.76527	-0.43502	2.157501
	Best	1	S_K=5_201-203-204-401-402_A42	0.319963	74.81604	-2.26684	2.010387

Table A7.2. Representative GFM placement outcomes in the simplified 14-generator NEM model.

Case	GFM placement	Approximate damping ratio	Main interpretation
Baseline	No GFM	About 28.6%	Reference dominant inter-area mode
Best one-GFM case	Bus 201 (NSW)	About 39.0%	Strong damping improvement because the GFM occupies an electrically influential NSW location and disrupts the compact NSW negative cluster
Weak one-GFM case	Bus 402 (QLD)	About 29.2%	Only minor improvement because the modal structure remains close to the baseline case
Best two-GFM case	Buses 201 and 401	About 36.3%	Cross-area placement improves damping by reshaping the inter-area mode more effectively
Weak two-GFM case	Buses 401 and 402 (QLD)	About 29.9%	Limited improvement because the placement does not significantly alter the dominant modal structure





(a) (b)

Figure A7.17. Inter-area oscillation study of 0-8 GFM placements for Mode 1 in the simplified 14-generator NEM model when the disturbance is applied to Bus 410: (a) eigenvalues; and (b) damping ratios.

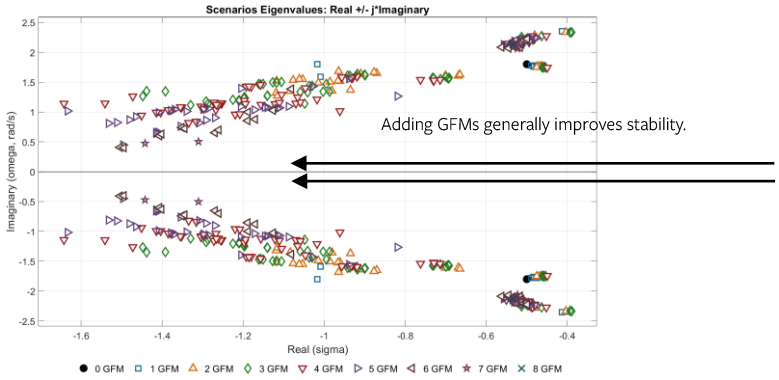


Figure A7.18. Inter-area oscillation study of 0-8 GFM placements for Mode 2 in the simplified 14-generator NEM model when the disturbance is applied to Bus 410.

Table A7.3. Best- and worst-case 0-8 GFM placements for Mode 1 in the simplified 14-generator NEM model for the Bus 410 disturbance case.

K	Rank	Kind	Mode	ScenarioID including GFM placement	Frequency	Damping %	Eigen (Real)	Eigen ($\lvert I_m \rvert$)
0	NA		1	S00_BASELINE_A42	0.382425	15.49412	-0.37685	2.402847
1	Worst		1	S_K=1_404_A42	0.373042	17.00346	-0.40443	2.343892
	Best		1	S_K=1_401_A42	0.508564	43.79987	-1.55686	3.195402
2	Worst		1	S_K=2_403-404_A42	0.371466	16.04165	-0.37932	2.33399
	Best		1	S_K=2_203-401_A42	0.47742	49.43574	-1.70597	2.999718
3	Worst		1	S_K=3_402-403-404_A42	0.370453	15.78031	-0.37197	2.327625
	Best		**1**	**S_K=3_201-402-404_A42**	**0.36206**	**74.62588**	**-2.55035**	**2.27489**
4	Worst		1	S_K=4_401-402-403-404_A42	0.370824	16.3465	-0.38606	2.329956
	Best		1	S_K=4_201-204-402-404_A42	0.411733	73.05664	-2.7678	2.586995

5	Worst	1	S_K=5_203-401-402-403-404_A42	0.368578	18.70973	-0.44108	2.315844
	Best	1	S_K=5_201-202-204-402-404_A42	0.447308	70.83233	-2.82022	2.810519
6	Worst	1	S_K=6_202-203-204-402-403-404_A42	0.34833	21.17233	-0.47413	2.188622
	Best	1	S_K=6_201-202-203-204-402-404_A42	0.467836	69.50461	-2.84171	2.9395
7	Worst	1	S_K=7_202-203-204-401-402-403-404_A42	0.344075	23.06885	-0.51255	2.161887
	Best	1	S_K=7_201-202-203-204-402-403-404_A42	0.69962	47.53702	-2.37518	4.395842
8	NA	1	S_K=8_201-202-203-204-401-402-403-404_A42	0.860522	28.3877	-1.60072	5.406819

Table A7.4. Best- and worst-case 0-7 GFM placements for Mode 2 in the simplified 14-generator NEM model for the Bus 410 disturbance case.

K	RankKind	Mode	ScenarioID including GFM placement	Frequency	Damping %	Eigen (Real)	Eigen ($\lvert I_m \rvert$)
0	NA	2	S00_BASELINE_A42	0.286563	26.75372	-0.49993	1.800528
1	Worst	2	S_K=1_403_A42	0.372438	16.84975	-0.40002	2.340097
	Best	2	S_K=1_404_A42	0.253168	53.57701	-1.00934	1.590701
2	Worst	2	S_K=2_401-402_A42	0.371858	17.00455	-0.40318	2.336453
	Best	2	S_K=2_403-404_A42	0.202479	65.92169	-1.11532	1.272213
3	Worst	2	S_K=3_401-402-404_A42	0.371511	16.44383	-0.38914	2.334272
	Best	2	S_K=3_204-403-404_A42	0.177866	76.55311	-1.32971	1.117565
4	Worst	2	S_K=4_203-401-402-403_A42	0.361845	19.48708	-0.45171	2.273539
	Best	2	S_K=4_204-402-403-404_A42	0.130321	85.23541	-1.33457	0.818831
5	Worst	2	S_K=5_204-401-402-403-404_A42	0.356701	20.76884	-0.47585	2.241218
	Best	2	S_K=5_201-204-402-403-404_A42	0.071396	95.78988	-1.49669	0.448594
6	Worst	2	S_K=6_202-203-401-402-403-404_A42	0.35407	21.8851	-0.49897	2.224687
	Best	2	S_K=6_202-203-204-402-403-404_A42	0.063736	96.59367	-1.49481	0.400465
7	Worst	2	S_K=7_201-203-204-401-402-403-404_A42	0.343615	23.17958	-0.51446	2.158997
	Best	2	S_K=7_201-202-203-204-401-403-404_A42	0.07533	95.0159	-1.4425	0.473312

A.8 Model use, workflow, and availability

The modelling workflow used in this project was developed through a staged process combining benchmark-system studies, partner-supported study files, and project-specific automation. The simplified 14-generator Australian/NEM system and the associated automation workflow were used as the main research platform for system-level studies. The SMIB benchmark provided by Powerlink was used for early DSATools-based modelling and validation, while the Kundur system was used as an established benchmark for multi-machine oscillation analysis. This subsection therefore clarifies the development context, provenance, and practical availability of the principal models and workflows used in the project.

In terms of availability, the project does not claim unrestricted public release of all study files. Some components of the work depend on partner-provided benchmark material and on commercial software environments such as PSSE, DSATools, and PowerWorld. The workflow, analytical approach, and benchmark logic are therefore reproducible in principle, but direct redistribution of all model files should remain subject to relevant permissions and software access conditions.

A.9 Key lessons learned from the research process

This subsection summarises the principal methodological and technical lessons that emerged from the research process. These lessons are included not as additional results, but as concise reflections on the modelling, validation, and interpretation issues that shaped the project and informed its final conclusions.

1. Lesson 1: Renewable integration studies should not stop at steady-state feasibility. The early 14-generator studies showed that acceptable power-flow results can coexist with less satisfactory post-disturbance oscillatory behaviour.

2. Lesson 2: GFM modelling studies require careful validation. Early controller and transient-simulation issues were not incidental; resolving them was necessary before meaningful small-signal and time-domain conclusions could be drawn.

3. Lesson 3: Cross-platform validation is essential. Broad consistency across PSSE, DSATools, and PowerWorld Simulator increased confidence in the findings. Observed discrepancies highlighted where controller interpretation requires care.

4. Lesson 4: System-level deployment questions require modal interpretation, not damping ratio alone. As the project progressed to multiple-GFM placement studies, participation, clustering, and opposition measures became essential for explaining why some placements worked well and others did not.

A.10 Relation of project outcomes to future research

The project has established a credible platform for future research on larger and more complex Australian-relevant systems. Possible future extensions include broader inter-area mode coverage, disturbance-location sensitivity, deeper tuning studies, and structured comparison of GFMs with synchronous condensers and combined GFM-BESS arrangements. These extensions would build on the project's current outcomes rather than alter its central conclusions.

RACE for 2030

RELIABLE
AFFORDABLE
CLEAN
ENERGY

info@racefor2030.com.au

UTS
L10 10/235 Jones St Ultimo,
NSW 2007 Australia

ABN 46 640 317 559

Australian Government
Department of Industry, Science and Resources

Cooperative Research Centres Program